

## Lehigh University Lehigh Preserve

---

### Theses and Dissertations

---

1997

# Parallel shear flows of two superimposed viscoelastic fluids

Mukaddes Selviboy  
*Lehigh University*

Follow this and additional works at: <http://preserve.lehigh.edu/etd>

---

### Recommended Citation

Selviboy, Mukaddes, "Parallel shear flows of two superimposed viscoelastic fluids" (1997). *Theses and Dissertations*. Paper 495.

This Thesis is brought to you for free and open access by Lehigh Preserve. It has been accepted for inclusion in Theses and Dissertations by an authorized administrator of Lehigh Preserve. For more information, please contact [preserve@lehigh.edu](mailto:preserve@lehigh.edu).

Selviboy,  
Mukaddes

Parallel Shear  
Flows of Two

---

Superimposed  
Viscoelastic Fluids

June 1, 1997

# **Parallel Shear Flows of Two Superimposed Viscoelastic Fluids**

by

Mukaddes Selviboy

A Thesis

---

Presented to the Graduate and Research Committee

of Lehigh University

in Candidacy for the Degree of

Master of Science

in

Applied Mathematics

in the Department of Mechanical Engineering and Mechanics

Lehigh University  
May 1997

This thesis is accepted and approved in partial fulfillment of the requirements for the master of Science.

4/30/97

Date

---

Thesis Advisor  
Prof. Jacob Y. Kazakia

Chairperson of Department  
Prof. Charles R. Smith

# TABLE OF CONTENTS

	<b>Page numbers</b>
List of Tables	v
List of Figures	vi
Abstract	1
Chapter 1. Introduction	3
Chapter 2. Basic Equations	7
Chapter 3. Shear Flow of Two Newtonian Fluids	14
3a. Parallel Plates	14
3b. Circular Cylinder	18
Chapter 4. Shear Flow of Two Upper Convected Maxwell Fluids	22
Chapter 5. Flow of Two Giesekus Type Viscoelastic Fluids	28
Chapter 6. Conclusion	42

Figures	43
Tables	82
References	83
Appendix	85

---

---

## LIST OF TABLES

*TABLE 1.* Summary of flow characteristics of the examples studied.

## LIST OF FIGURES

*FIGURE 1.* Parallel plates geometry.

*FIGURE 2.* The components of the stress tensor  $S$ .

*FIGURE 3.* A relationship of velocity gradient  $\chi_1$  and  $\chi_2$  with the interface velocity.

*FIGURE 4.* The velocity gradients  $\chi_i$  in the two layers as functions of the network viscosity  $\eta$  of the upper layer for values of the network mobility parameter  $\alpha$  between 0.1 and 0.5. Case A where  $We_1 = We_2 = 1$ ,  $d_1 = d_2 = 0.5$ . The Newtonian viscosities are zero, the network viscosity of the lower layer is fixed at 1. a)  $\chi_1$  vs.  $\eta_2$   
b)  $\chi_2$  vs.  $\eta_2$

*FIGURE 5.* The shear stress  $\tau_i$  in the two layers as functions of the network viscosity  $\eta$  of the upper layer for values of the network mobility parameter  $\alpha$  between 0.1 and 0.5. Case A where  $We_1 = We_2 = 1$ ,  $d_1 = d_2 = 0.5$ . The Newtonian viscosities are zero, the network viscosity of the lower layer is fixed at 1.

*FIGURE 6.* The first normal stress differences  $n_{1i}$  in the two layers as functions of the network viscosity  $\eta$  of the upper layer for values of the network mobility parameter  $\alpha$  between 0.1 and 0.5. Case A where  $We_1 = We_2 = 1$ ,  $d_1 = d_2 = 0.5$ . The Newtonian viscosities are zero, the network viscosity of the lower layer is fixed at 1.  
a)  $n_{11}$  vs.  $\eta_2$     b)  $n_{12}$  vs.  $\eta_2$

*FIGURE 7.* The second normal stress differences  $n_{2i}$  in the two layers as functions of the network viscosity  $\eta$  of the upper layer for values of the network mobility parameter  $\alpha$  between 0.1 and 0.5. Case A where  $We_1 = We_2 = 1$ ,  $d_1 = d_2 = 0.5$ . The Newtonian viscosities are zero, the network viscosity of the lower layer is fixed at 1.  
a)  $n_{21}$  vs.  $\eta_2$     b)  $n_{22}$  vs.  $\eta_2$ .



*FIGURE 8.* The velocity gradients  $\chi_i$  in the two layers as functions of the network viscosity  $\eta$  of the upper layer for values of the network mobility parameter  $\alpha$  between 0.1 and 0.5. Case B where  $We_1 = 1$   $We_2 = 0.2$ ,  $d_1 = d_2 = 0.5$ . The Newtonian viscosities are zero, the network viscosity of the lower layer is fixed at 1.

a)  $\chi_1$  vs.  $\eta_2$     b)  $\chi_2$  vs.  $\eta_2$

*FIGURE 9.* The shear stress  $\tau_i$  in the two layers as functions of the network viscosity  $\eta$  of the upper layer for values of the network mobility parameter  $\alpha$  between 0.1 and 0.5. Case B where  $We_1 = 1$   $We_2 = 0.2$ ,  $d_1 = d_2 = 0.5$ . The Newtonian viscosities are zero, the network viscosity of the lower layer is fixed at 1.

*FIGURE 10.* The first normal stress differences  $n_{1i}$  in the two layers as functions of the network viscosity  $\eta$  of the upper layer for values of the network mobility parameter  $\alpha$  between 0.1 and 0.5. Case B where  $We_1 = 1$   $We_2 = 0.2$ ,  $d_1 = d_2 = 0.5$ . The Newtonian viscosities are zero, the network viscosity of the lower layer is fixed at 1.

a)  $n_{11}$  vs.  $\eta_2$     b)  $n_{12}$  vs.  $\eta_2$

*FIGURE 11.* The second normal stress differences  $n_{2i}$  in the two layers as functions of the network viscosity  $\eta$  of the upper layer for values of the network mobility parameter  $\alpha$  between 0.1 and 0.5. Case B where  $We_1 = 1$   $We_2 = 0.2$ ,  $d_1 = d_2 = 0.5$ . The Newtonian viscosities are zero, the network viscosity of the lower layer is fixed at 1.

1. a)  $n_{21}$  vs.  $\eta_2$     b)  $n_{22}$  vs.  $\eta_2$

*FIGURE 12.* The velocity gradients  $\chi_i$  in the two layers as functions of the network viscosity  $\eta$  of the upper layer for values of the network mobility parameter  $\alpha$  between 0.1 and 0.5. Case C where  $We_1 = 1$   $We_2 = 2$ ,  $d_1 = d_2 = 0.5$ . The Newtonian viscosities are zero, the network viscosity of the lower layer is fixed at 1.

a)  $\chi_1$  vs.  $\eta_2$     b)  $\chi_2$  vs.  $\eta_2$

*FIGURE 13.* The shear stress  $\tau_i$  in the two layers as functions of the network viscosity  $\eta$  of the upper layer for values of the network mobility parameter  $\alpha$  between 0.1 and 0.5. Case C where  $We_1 = 1$   $We_2 = 2$ ,  $d_1 = d_2 = 0.5$ . The Newtonian viscosities are zero, the network viscosity of the lower layer is fixed at 1.

*FIGURE 14.* The first normal stress differences  $n_{1i}$  in the two layers as functions of the network viscosity  $\eta$  of the upper layer for values of the network mobility parameter  $\alpha$  between 0.1 and 0.5. Case C where  $We_1 = 1$   $We_2 = 2$ ,  $d_1 = d_2 = 0.5$ . The Newtonian viscosities are zero, the network viscosity of the lower layer is fixed at 1.

a)  $n_{11}$  vs.  $\eta_2$     b)  $n_{12}$  vs.  $\eta_2$

*FIGURE 15.* The second normal stress differences  $n_{2i}$  in the two layers as functions of the network viscosity  $\eta$  of the upper layer for values of the network mobility parameter  $\alpha$  between 0.1 and 0.5. Case C where  $We_1 = 1$   $We_2 = 2$ ,  $d_1 = d_2 = 0.5$ . The Newtonian viscosities are zero, the network viscosity of the lower layer is fixed at 1.

1. a)  $n_{21}$  vs.  $\eta_2$     b)  $n_{22}$  vs.  $\eta_2$

*FIGURE 16.* The velocity gradients  $\chi_i$  in the two layers as functions of the network viscosity  $\eta$  of the upper layer for values of the network mobility parameter  $\alpha$  between 0.1 and 0.5. Case D where  $We_1 = We_2 = 1$ ,  $d_1 = 0.1$   $d_2 = 0.9$ . The Newtonian viscosities are zero, the network viscosity of the lower layer is fixed at 1.

a)  $\chi_1$  vs.  $\eta_2$     b)  $\chi_2$  vs.  $\eta_2$

*FIGURE 17.* The shear stress  $\tau_i$  in the two layers as functions of the network viscosity  $\eta$  of the upper layer for values of the network mobility parameter  $\alpha$  between 0.1 and 0.5. Case D where  $We_1 = We_2 = 1$ ,  $d_1 = 0.1$   $d_2 = 0.9$ . The Newtonian viscosities are zero, the network viscosity of the lower layer is fixed at 1.

*FIGURE 18.* The first normal stress differences  $n_{1i}$  in the two layers as functions of the network viscosity  $\eta$  of the upper layer for values of the network mobility parameter

$\alpha$  between 0.1 and 0.5. Case D where  $We_1 = We_2 = 1$ ,  $d_1 = 0.1$   $d_2 = 0.9$ . The Newtonian viscosities are zero, the network viscosity of the lower layer is fixed at 1.

a)  $n_{11}$  vs.  $\eta_2$     b)  $n_{12}$  vs.  $\eta_2$

*FIGURE 19.* The second normal stress differences  $n_{2i}$  in the two layers as functions of the network viscosity  $\eta$  of the upper layer for values of the network mobility parameter  $\alpha$  between 0.1 and 0.5. Case D where  $We_1 = We_2 = 1$ ,  $d_1 = 0.1$   $d_2 = 0.9$ . The Newtonian viscosities are zero, the network viscosity of the lower layer is fixed at 1. a)  $n_{21}$  vs.  $\eta_2$     b)  $n_{22}$  vs.  $\eta_2$

*FIGURE 20.* The velocity gradients  $\chi_i$  in the two layers as functions of the network viscosities  $\eta$  of the upper layer for values of the network mobility parameter  $\alpha$  between 0.1 and 0.5. Case E where  $We_1 = 1$   $We_2 = 0.2$ ,  $d_1 = 0.1$   $d_2 = 0.9$ . The Newtonian viscosities are zero, the network viscosity of the lower layer is fixed at 1.

a)  $\chi_1$  vs.  $\eta_2$     b)  $\chi_2$  vs.  $\eta_2$

*FIGURE 21.* The shear stress  $\tau_i$  in the two layers as functions of the network viscosities  $\eta$  of the upper layer for values of the network mobility parameter  $\alpha$  between 0.1 and 0.5. Case E where  $We_1 = 1$   $We_2 = 0.2$ ,  $d_1 = 0.1$   $d_2 = 0.9$ . The Newtonian viscosities are zero, the network viscosity of the lower layer is fixed at 1.

*FIGURE 22.* The first normal stress differences  $n_{1i}$  in the two layers as functions of the network viscosity  $\eta$  of the upper layer for values of the network mobility parameter  $\alpha$  between 0.1 and 0.5. Case E where  $We_1 = 1$   $We_2 = 0.2$ ,  $d_1 = 0.1$   $d_2 = 0.9$ . The Newtonian viscosities are zero, the network viscosity of the lower layer is fixed at 1.

a)  $n_{11}$  vs.  $\eta_2$     b)  $n_{12}$  vs.  $\eta_2$

*FIGURE 23.* The second normal stress differences  $n_{2i}$  in the two layers as functions of the network viscosity  $\eta$  of the upper layer for values of the network mobility parameter  $\alpha$  between 0.1 and 0.5. Case E where  $We_1 = 1$   $We_2 = 0.2$ ,  $d_1 = 0.1$

$d_2 = 0.9$ . The Newtonian viscosities are zero, the network viscosity of the lower layer is fixed at 1. a)  $n_{21}$  vs.  $\eta_2$     b)  $n_{22}$  vs.  $\eta_2$

*FIGURE 24.* The velocity gradients  $\chi_i$  in the two layers as functions of the network viscosity  $\eta$  of the upper layer for values of the network mobility parameter  $\alpha$  between 0.1 and 0.5. Case F where  $We_1 = 1$   $We_2 = 2$ ,  $d_1 = 0.1$   $d_2 = 0.9$ . The Newtonian viscosities are zero, the network viscosity of the lower layer is fixed at 1.

a)  $\chi_1$  vs.  $\eta_2$     b)  $\chi_2$  vs.  $\eta_2$

*FIGURE 25.* The shear stress  $\tau_i$  in the two layers as functions of the network viscosity  $\eta$  of the upper layer for values of the network mobility parameter  $\alpha$  between 0.1 and 0.5. Case F where  $We_1 = 1$   $We_2 = 2$ ,  $d_1 = 0.1$   $d_2 = 0.9$ . The Newtonian viscosities are zero, the network viscosity of the lower layer is fixed at 1.

*FIGURE 26.* The first normal stress differences  $n_{1i}$  in the two layers as functions of the network viscosity  $\eta$  of the upper layer for values of the network mobility parameter  $\alpha$  between 0.1 and 0.5. Case F where  $We_1 = 1$   $We_2 = 2$ ,  $d_1 = 1$   $d_2 = 0.9$ . The Newtonian viscosities are zero, the network viscosity of the lower layer is fixed at 1.

a)  $n_{11}$  vs.  $\eta_2$     b)  $n_{12}$  vs.  $\eta_2$

*FIGURE 27.* The second normal stress differences  $n_{2i}$  in the two layers as functions of the network viscosity  $\eta$  of the upper layer for values of the network mobility parameter  $\alpha$  between 0.1 and 0.5. Case F where  $We_1 = 1$   $We_2 = 2$ ,  $d_1 = 0.1$   $d_2 = 0.9$ . The Newtonian viscosities are zero, the network viscosity of the lower layer is fixed at 1.

a)  $n_{21}$  vs.  $\eta_2$     b)  $n_{22}$  vs.  $\eta_2$

*FIGURE 28.* The velocity gradients  $\chi_i$  in the two layers as functions of the network viscosity  $\eta$  of the upper layer for values of the network mobility parameter  $\alpha$  between

0.1 and 0.5. Case G where  $We_1 = We_2 = 1$ ,  $d_1 = 0.9$   $d_2 = 0.1$ . The Newtonian viscosities are zero, the network viscosity of the lower layer is fixed at 1.

a)  $\chi_1$  vs.  $\eta_2$     b)  $\chi_2$  vs.  $\eta_2$

*FIGURE 29.* The shear stress  $\tau_i$  in the two layers as functions of the network viscosity  $\eta$  of the upper layer for values of the network mobility parameter  $\alpha$  between 0.1 and 0.5. Case G where  $We_1 = We_2 = 1$ ,  $d_1 = 0.9$   $d_2 = 0.1$ . The Newtonian viscosities are zero, the network viscosity of the lower layer is fixed at 1.

*FIGURE 30.* The first normal stress differences  $n_{1i}$  in the two layers as functions of the network viscosity  $\eta$  of the upper layer for values of the network mobility parameter  $\alpha$  between 0.1 and 0.5. Case G where  $We_1 = We_2 = 1$ ,  $d_1 = 0.9$   $d_2 = 0.1$ . The Newtonian viscosities are zero, the network viscosity of the lower layer is fixed at 1.

a)  $n_{11}$  vs.  $\eta_2$     b)  $n_{12}$  vs.  $\eta_2$

*FIGURE 31.* The second normal stress differences  $n_{2i}$  in the two layers as functions of the network viscosity  $\eta$  of the upper layer for values of the network mobility parameter  $\alpha$  between 0.1 and 0.5. Case G where  $We_1 = We_2 = 1$ ,  $d_1 = 0.9$   $d_2 = 0.1$ . The Newtonian viscosities are zero, the network viscosity of the lower layer is fixed at 1.

1. a)  $n_{21}$  vs.  $\eta_2$     b)  $n_{22}$  vs.  $\eta_2$

*FIGURE 32.* The velocity gradients  $\chi_i$  in the two layers as functions of the network viscosity  $\eta$  of the upper layer for values of the network mobility parameter  $\alpha$  between 0.1 and 0.5. Case H where  $We_1 = 1$   $We_2 = 0.2$ ,  $d_1 = 0.9$   $d_2 = 0.1$ . The Newtonian viscosities are zero, the network viscosity of the lower layer is fixed at 1.

a)  $\chi_1$  vs.  $\eta_2$     b)  $\chi_2$  vs.  $\eta_2$

*FIGURE 33.* The shear stress  $\tau_i$  in the two layers as functions of the network viscosity  $\eta$  of the upper layer for values of the network mobility parameter  $\alpha$  between

0.1 and 0.5. Case H where  $We_1 = 1$   $We_2 = 0.2$ ,  $d_1 = 0.9$   $d_2 = 0.1$ . The Newtonian viscosities are zero, the network viscosity of the lower layer is fixed at 1.

*FIGURE 34.* The first normal stress differences  $n_{1i}$  in the two layers as functions of the network viscosity  $\eta$  of the upper layer for values of the network mobility parameter  $\alpha$  between 0.1 and 0.5. Case H where  $We_1 = 1$   $We_2 = 0.2$ ,  $d_1 = 0.9$   $d_2 = 0.1$ . The Newtonian viscosities are zero, the network viscosity of the lower layer is fixed at 1.

a)  $n_{11}$  vs.  $\eta_2$     b)  $n_{12}$  vs.  $\eta_2$

*FIGURE 35.* The second normal stress differences  $n_{2i}$  in the two layers as functions of the network viscosity  $\eta$  of the upper layer for values of the network mobility parameter  $\alpha$  between 0.1 and 0.5. Case H where  $We_1 = 1$   $We_2 = 0.2$ ,  $d_1 = 0.9$   $d_2 = 0.1$ . The Newtonian viscosities are zero, the network viscosity of the lower layer is fixed at 1.

a)  $n_{21}$  vs.  $\eta_2$     b)  $n_{22}$  vs.  $\eta_2$

*FIGURE 36.* The velocity gradients  $\chi_i$  in the two layers as functions of the network viscosity  $\eta$  of the upper layer for values of the network mobility parameter  $\alpha$  between 0.1 and 0.5. Case I where  $We_1 = 1$   $We_2 = 2$ ,  $d_1 = 0.9$   $d_2 = 0.1$ . The Newtonian viscosities are zero, the network viscosity of the lower layer is fixed at 1

a)  $\chi_1$  vs.  $\eta_2$     b)  $\chi_2$  vs.  $\eta_2$

*FIGURE 37.* The shear stress  $\tau_i$  in the two layers as functions of the network viscosity  $\eta$  of the upper layer for values of the network mobility parameter  $\alpha$  between 0.1 and 0.5. Case I where  $We_1 = 1$   $We_2 = 2$ ,  $d_1 = 0.9$   $d_2 = 0.1$ . The Newtonian viscosities are zero, the network viscosity of the lower layer is fixed at 1.

*FIGURE 38.* The first normal stress differences  $n_{1i}$  in the two layers as functions of the network viscosity  $\eta$  of the upper layer for values of the network mobility parameter

$\alpha$  between 0.1 and 0.5. Case I where  $We_1 = 1$   $We_2 = 2$ ,  $d_1 = 0.9$   $d_2 = 0.1$ . The Newtonian viscosities are zero, the network viscosity of the lower layer is fixed at 1.

a)  $n_{11}$  vs.  $\eta_2$     b)  $n_{12}$  vs.  $\eta_2$

*FIGURE 39.* The second normal stress differences  $n_{2i}$  in the two layers as functions of the network viscosity  $\eta$  of the upper layer for values of the network mobility parameter  $\alpha$  between 0.1 and 0.5. Case I where  $We_1 = 1$   $We_2 = 2$ ,  $d_1 = 0.9$   $d_2 = 0.1$ . The Newtonian viscosities are zero, the network viscosity of the lower layer is fixed at 1.

a)  $n_{21}$  vs.  $\eta_2$     b)  $n_{22}$  vs.  $\eta_2$

## ABSTRACT

In this thesis we investigate the shear flow of two superimposed viscoelastic fluids under steady state conditions.

Several important applications of such flows include lubricated transport of crude oil through pipelines, co-extrusion of polymeric liquids in foaming composite materials, and coating of liquid layers to a substrate.

We consider the general case for which each layer has a different density, viscosity and relaxation time. The layer thickness is an additional parameter. Both geometries of parallel plates and cylindrical pipe are considered.

The closed form solutions for the case of Newtonian fluids are derived for completeness. The Upper Convected Maxwell fluid and The Oldroyd -B model are used to describe the viscoelastic behavior of dilute solutions of polymeric molecules. Closed form solutions for these fluids are also derived.

Concentrated solutions of polymers which exhibit second normal stress differences and shear thinning can be described by a more complex viscoelastic model known as the Giesekus model. Solutions for the Couette flow of two superimposed fluids described by the Giesekus model are obtained numerically and the effect of the variation of some of the parameters on the flow is investigated.

As expected, the second normal stress difference increases for increasing values of the mobility parameter  $\alpha$ . In addition, increased Weissenberg numbers produce higher second normal stress differences.

In the cases where one of the layers is much thinner than the other, we conclude that the nondimensional velocity gradient in the thick layer remains very



close to 1 for all values of the mobility parameter, provided that its viscosity is less than that of the thin layer.

## 1. INTRODUCTION

Shear flows of immiscible multiple-component systems have attracted the attention of many researchers, in recent years. Such flows have many practical applications in the processing and transport of materials. Examples include lubricated transport of crude oil through pipelines; co-extrusion of polymeric liquids in forming composite materials with unique mechanical and optical properties; and coating of multiple liquid layers to a substrate.

In this thesis some of the flows are analyzed under steady state conditions. We concentrate on two layered shear flows. Both geometries of parallel plane and circular cylinder are being considered. We start our discussion by focusing on the shear flow of two layers of viscous Newtonian fluids superimposed in a parallel plate geometry. Each layer has its own viscosity and density. The thickness ratio is another parameter of the problem. This problem has a rather simple closed form solution, in either the Couette or Poiseuille flow case. Similarly the flow of two concentric cylindrical fluids within a pipe under pressure gradient is studied and closed form solutions are listed.

We next consider the case when the fluids involved are viscoelastic. Many of the practical problems mentioned earlier do indeed involve dilute solutions of polymer molecules. In some cases one may even have to consider concentrated solutions and melts of flexible polymer molecules. Both dilute solutions and melts can possess first normal stress differences. This is the difference between the normal stress in the direction of the flow and the normal stress in the direction of the velocity gradients. Of course for a Newtonian fluid both normal stresses are equal to the additive inverse of the pressure. Both dilute solutions and melts may exhibit shear

thinning . This is a manifestation of shear rate dependence of the apparent viscosity due to the nonlinear relation between shear rate and shear stress.

The shear thinning of dilute solutions is usually light , however melts manifest a strong shear thinning as well as second normal stress differences. Two models are used for the description of dilute solutions of polymeric molecules. One is the Upper Convected Maxwell (UCM) fluid ,which has two material parameters: the zero shear viscosity and the relaxation time. The influence of viscoelasticity on the flow is characterized by the Weissenberg number which is the product of the relaxation time and a typical velocity gradient. Since in this thesis we consider steady state problem, the Deborah number does not enter our discussion.

We generalize the (UCM) model equation by considering an additional solvent viscosity. This is the Oldroyd-B model which can be derived from a molecular model in which the polymer molecule is idealized as an infinitely extensible Hookean spring connecting two Brownian beads [6]. The model has been shown to give predictions in simple shear flows that are in qualitative agreement with laboratory measurements done for Boger fluids.

As we mentioned earlier, polymer melts and concentrated solutions of polymers exhibit second normal stress differences and shear thinning. There are several viscoelastic models predicting this type of behavior [1], [7]-[10]. A detailed summary of these models is given by R.G. Larson [5] .

In this thesis we concentrate on the Giesekus model for melts. For simplicity we use the single mode form of this model, which is capable to predict the second normal stress difference as well as shear thinning.

With two such fluids undergoing shear flow there is a great number of possible configurations. Several of these are examined and analyzed in the present thesis. A complete study of the problem would require a stability analysis which would predict which of these possible configurations would be stable under small disturbances and hence good candidates for processes of practical importance. This, more difficult problem, is not treated here but it will be considered later.

The organization of this thesis is as follows. In chapter 2, we describe the basic equations to be used. We list the continuity and momentum equation together with the constitutive equation for a Newtonian fluid. For a viscoelastic fluid of UCM and Oldroyd-B type. The constitutive equation for Giesekus type fluids are also presented and nondimensionalized. Stresses are measured relative to a reference shear stress. In this chapter we also summarize the boundary and interfacial conditions. In chapter 3 we describe the solution of two superimposed Newtonian fluids between two parallel plates. Couette flow with zero pressure gradients is considered. We also study the Poiseuille problem when the two fluids are in the form of two concentric cylinders within a circular pipe.

In chapter 4 we considered the case of two Superimposed Viscoelastic fluids of the UCM type between two parallel plates. Again both Couette flow with zero pressure gradient and Poiseuille flow with non zero pressure gradient are considered.

In chapter 5 we study the same problem for zero pressure gradient when both of the fluids are represented the a single mode Giesekus type constitutive equation. The nonlinear character of this last problem requires a numerical approach to obtain the basic flow characteristic.

In the geometry studied here in each layer there is only one non zero velocity component and this is a function of the shear coordinate which is perpendicular to the plates. The constitutive and momentum equation predict that the velocity gradients in the layers are constants and they are used to express all stresses in terms of these velocity gradients. Both velocity gradients are then written in terms of the velocity of the interface and finally the shear stress interfacial condition is used to determine this velocity and consequently all other variables. This last equation is nonlinear and an appropriate method is used to produce accurate solutions.

In chapter 6 we present our conclusion, based on this analysis of shear flows for various combinations of the material and geometric parameters.

---

## 2. BASIC EQUATIONS

In this work, we consider the flow of either a single fluid or that of a system of two superimposed fluids occupying the region between two rigid plates. In some cases, we consider the flow of two concentrically situated fluids inside a circular cylinder.

In the case of the parallel plates geometry, we consider a Cartesian coordinate system with the x and y axes on the lower plate. The x axis is in the direction of the flow and the z axis is in the direction perpendicular to the plates, as shown in figure 1.

We denote by

$$u_i, v_i, w_i, \quad i = 1, 2, \quad (2.1)$$

the velocity components of the flow. The index  $i=1$  corresponds to the lower fluid and  $i=2$  corresponds to the upper fluid. The densities  $\rho_1$  and  $\rho_2$  of the two fluids may be different but we make the assumption of incompressible flow and consequently the continuity equations for each fluid component are

$$\frac{\partial u_i}{\partial x} + \frac{\partial v_i}{\partial y} + \frac{\partial w_i}{\partial z} = 0. \quad (2.2)$$

The corresponding momentum equations for each component fluid of the system are given by

$$\rho g_x + \frac{\partial \sigma_{xx}}{\partial x} + \frac{\partial \tau_{yx}}{\partial y} + \frac{\partial \tau_{zx}}{\partial z} = \rho \left( \frac{\partial u}{\partial t} + u \frac{\partial u}{\partial x} + v \frac{\partial u}{\partial y} + w \frac{\partial u}{\partial z} \right), \quad (2.3)$$

$$\rho g_y + \frac{\partial \tau_{xy}}{\partial x} + \frac{\partial \sigma_{yy}}{\partial y} + \frac{\partial \tau_{zy}}{\partial z} = \rho \left( \frac{\partial v}{\partial t} + u \frac{\partial v}{\partial x} + v \frac{\partial v}{\partial y} + w \frac{\partial v}{\partial z} \right), \quad (2.4)$$

$$\rho g_z + \frac{\partial \tau_{xz}}{\partial x} + \frac{\partial \tau_{yz}}{\partial y} + \frac{\partial \sigma_{zz}}{\partial z} = \rho \left( \frac{\partial w}{\partial t} + u \frac{\partial w}{\partial x} + v \frac{\partial w}{\partial y} + w \frac{\partial w}{\partial z} \right), \quad (2.5)$$

where  $\sigma_{xx}, \sigma_{yy}, \sigma_{zz}, \tau_{xy}, \tau_{xz}, \tau_{yz}$  are the components of the stress tensor  $\underline{S}$ .

$$\underline{S} = \begin{bmatrix} \sigma_{xx} & \tau_{xy} & \tau_{xz} \\ \tau_{xy} & \sigma_{yy} & \tau_{yz} \\ \tau_{xz} & \tau_{yz} & \sigma_{zz} \end{bmatrix}. \quad (2.6)$$

The stress at a point is specified by the six components where  $\sigma$  has been used to denote a normal stress and  $\tau$  has been used to denote a shear stress.

Figure 2 illustrates the components of the stress tensor  $\underline{S}$ . In the case of Newtonian Fluid, the shear stresses are

$$\tau_{xy} = \mu \left( \frac{\partial v}{\partial x} + \frac{\partial u}{\partial y} \right), \quad (2.7)$$

$$\tau_{yz} = \mu \left( \frac{\partial v}{\partial z} + \frac{\partial w}{\partial y} \right), \quad (2.8)$$

$$\tau_{zx} = \mu \left( \frac{\partial w}{\partial x} + \frac{\partial u}{\partial z} \right), \quad (2.9)$$

and normal stress are given by :

$$\sigma_{xx} = -p + 2\mu \frac{\partial u}{\partial x}, \quad (2.10)$$

$$\sigma_{yy} = -p + 2\mu \frac{\partial v}{\partial y}, \quad (2.11)$$

$$\sigma_{zz} = -p + 2\mu \frac{\partial w}{\partial z}, \quad (2.12)$$

where  $p$  is the pressure in the fluid.

Equations (2.7) through (2.12) can be summarized by the tensor equation

$$\underline{S} = -p\underline{I} + \mu[\underline{\nabla} \underline{u} + (\underline{\nabla} \underline{u})^T], \quad (2.13)$$

where  $\underline{I}$  is the identity tensor and

$$(\underline{\nabla} \underline{u})_{ij} = \frac{\partial u_i}{\partial x_j}. \quad (2.14)$$

Here we use the notation

$$u_1 = u, u_2 = v, u_3 = w. \quad (2.15)$$

In Chapter 4, we discuss the flow of upper convected Maxwell fluids. Consequently, we introduce here the constitutive equations describing the behavior of these fluids.

The stress tensor  $\underline{S}$  is related to the pressure  $p$  and to the "extra" stress  $\underline{T}$  by

$$\underline{S} = -p\underline{I} + \underline{T}, \quad (2.16)$$

The "extra" stress  $\underline{T}$  satisfies the differential equation

$$\underline{T} + \lambda \frac{D\underline{T}}{Dt} = \eta(\underline{\nabla} \underline{u} + \underline{\nabla} \underline{u})^T, \quad (2.17)$$



where  $\lambda$  is the relaxation time and  $\eta$  is the viscosity and  $\frac{D}{Dt}$  denotes the upper convected time derivative.

$$\frac{D\underline{T}}{Dt} = \frac{\partial \underline{T}}{\partial t} + (\underline{u} \cdot \nabla) \underline{T} - \left[ \nabla \underline{u} \cdot \underline{T} + \underline{T} (\nabla \cdot \underline{u})^T \right], \quad (2.18)$$

where

$$(\underline{u} \cdot \nabla) = \left( u \frac{\partial}{\partial x} + v \frac{\partial}{\partial y} + w \frac{\partial}{\partial z} \right). \quad (2.19)$$

If equation (2.16) is modified to include the effect of a Newtonian viscosity

i.e.

$$\underline{S} = -p\underline{I} + \underline{T} + \mu (\nabla \underline{u} + \nabla \underline{u})^T \quad (2.20)$$

then one has the constitutive equation for the Oldroyd B type fluid which may be physically interpreted as a mixture of a viscoelastic fluid in a Newtonian solvent.

Another more general fluid to be considered here is the one introduced by Giesekus [1] which is capable to model second normal stress differences and also shear thinning behavior.

A set of constitutive equations for one special case of this fluid is

$$\underline{S} = \underline{T}^s + \underline{T} \quad (2.21)$$

where  $\underline{T}^s$  is the Newtonian solvent contribution

$$\underline{T}^s = -p\underline{I} + \mu_s [\nabla \underline{u} + (\nabla \underline{u})^T], \quad (2.22)$$

and  $\underline{T}$  is the viscoelastic stress contribution. In equation (2.22)  $\mu_s$  is the solvent viscosity.

The tensor  $\underline{T}$  satisfies the equation:

$$\underline{T} + \lambda \frac{D\underline{T}}{Dt} + \frac{\alpha\lambda}{\eta} \underline{T} \underline{T} = 2\eta \underline{D} \quad (2.23)$$

where  $\underline{D}$  is the rate of strain tensor given by

$$\underline{D} = \frac{1}{2} [ \underline{\nabla} \underline{u} + (\underline{\nabla} \underline{u})^T ] \quad (2.24)$$

and  $\alpha, \lambda, \eta$  are material parameters.

The time derivative  $\frac{D}{Dt}$  which appears in 2.23 is defined earlier by equation 2.18.

We would like to rewrite all of the equations presented in this section in nondimensional form. This will facilitate discussion in this sections to follow.

We measure all distances relative to do a reference length  $d_{ref}$ , i.e.

$$(\bar{x}, \bar{y}, \bar{z}) = (x, y, z)/d_{ref} \quad (2.25)$$

We measure velocities relative to a reference velocity  $U_{ref}$ , i.e.

$$(\bar{u}_i, \bar{v}_i, \bar{w}_i) = (u_i, v_i, w_i)/U_{ref} \quad (2.26)$$

We measure time relative to  $d_{ref}/U_{ref}$ , i.e.

$$\bar{t} = tU_{ref}/d_{ref}, \quad \bar{\lambda} = \lambda U_{ref}/d_{ref} \quad (2.27)$$

We measure viscosities and densities relative to a reference viscosity  $\mu_{ref}$  and reference density  $\rho_{ref}$ , i.e.

$$\bar{\mu} = \mu_i/\mu_{ref}, \quad \bar{\eta} = \eta_i/\mu_{ref}, \quad \bar{\rho} = \rho_i/\rho_{ref}. \quad (2.28)$$

Finally, we measure stresses relative to the reference shear stress  $\mu_{ref}U_{ref}/d_{ref}$ , i.e.

$$\bar{p} = pd_{ref}/\mu_{ref}U_{ref}, \quad (\bar{\underline{T}}, \bar{\underline{S}}) = (\underline{T}, \underline{S})d_{ref}/\mu_{ref}U_{ref}. \quad (2.29)$$

Using equations (2.25)-(2.29) and dropping the bars from the non dimensional variables we obtain the non dimensional form of the continuity equation as:

$$\frac{\partial u}{\partial x} + \frac{\partial v}{\partial y} + \frac{\partial w}{\partial z} = 0 . \quad (2.30)$$

and the non dimensional form of the momentum equations,

$$(Re_{ref}/Fr_{ref}^2)\rho g_x + \frac{\partial \sigma_{xx}}{\partial x} + \frac{\partial \tau_{yx}}{\partial y} + \frac{\partial \tau_{zx}}{\partial z} = Re_{ref}\rho \left( \frac{\partial u}{\partial t} + u \frac{\partial u}{\partial x} + v \frac{\partial u}{\partial y} + w \frac{\partial u}{\partial z} \right), \quad (2.31)$$

$$(Re_{ref}/Fr_{ref}^2)\rho g_y + \frac{\partial \tau_{xy}}{\partial x} + \frac{\partial \sigma_{yy}}{\partial y} + \frac{\partial \tau_{zy}}{\partial z} = Re_{ref}\rho \left( \frac{\partial v}{\partial t} + u \frac{\partial v}{\partial x} + v \frac{\partial v}{\partial y} + w \frac{\partial v}{\partial z} \right), \quad (2.32)$$

$$(Re_{ref}/Fr_{ref}^2)\rho g_z + \frac{\partial \tau_{xz}}{\partial x} + \frac{\partial \tau_{yz}}{\partial y} + \frac{\partial \sigma_{zz}}{\partial z} = Re_{ref}\rho \left( \frac{\partial w}{\partial t} + u \frac{\partial w}{\partial x} + v \frac{\partial w}{\partial y} + w \frac{\partial w}{\partial z} \right), \quad (2.33)$$

Here the reference Froude number is given by

$$Fr_{ref} = \frac{U_{ref}}{\sqrt{gd_{ref}}} \quad (2.34)$$

Where  $g$  is the gravitational acceleration. We point that  $g_x, g_y, g_z$  are nondimensionalized relative to the gravitational acceleration  $g$ .

In equations (2.31)-(2.33) the reference Reynold's number  $Re_{ref}$  is given by

$$Re_{ref} = \frac{\rho_{ref}U_{ref}d_{ref}}{\mu_{ref}} \quad (2.35)$$

In addition, the time derivative  $D/D_t$  which appears in (2.23) is still defined as earlier by equation (2.18). The non dimensional form of the constitutive equation of the Giesekus fluid (cf. equation 2.23) is

$$\underline{T} + w_e \frac{DT}{Dt} + \frac{\alpha}{\eta} w_e \underline{T} \underline{T} = \eta [ \underline{\nabla} \underline{u} + (\underline{\nabla} \underline{u})^T ] \quad (2.36)$$

where the Weissenberg number  $w_e$  is the non dimensional relaxation time  $\bar{\lambda}$  given by equation (2.27).

---

### 3. SHEAR FLOW OF TWO NEWTONIAN FLUIDS

In this section we summarize some known results about the simple shear of two different Newtonian fluids in contact.

The fluids are assumed to be immiscible so there is a sharp interface. Couette flow for parallel plates and the Poiseuille flow for both geometries of parallel plates and circular cylinder will be discussed.

#### 3a. Parallel Plates

Here we first consider the simple shear flow of two superimposed Newtonian fluids between two parallel plates separated by a distance  $d_0$ . The lower plate is stationary while the top plate moves with a velocity  $U$ . The only velocity component present is the one in the x-direction and it depends on  $z$  only so that

$$u_i = u_i(z) \tag{3.1}$$

and

$$v_i = w_i = 0, \quad i = 1, 2 \tag{3.2}$$

We choose  $U$  as  $U_{ref}$  and  $d_0$  as  $d_{ref}$ .

The lower fluid occupies the region defined by  $0 \leq z < d_1$  and the upper fluid occupies the region defined by  $d_1 \leq z < d_2$ . The index  $i = 1$  corresponds to the lower fluid and  $i = 2$  corresponds to the upper fluid.

In nondimensional form the boundary conditions are given by

$$u_1(0) = 0, \quad (3.3)$$

$$u_2(1) = 1 \quad (3.4)$$

and the interface conditions are

$$(\tau_{zx})_1 = (\tau_{zx})_2 \quad (3.5)$$

$$u_1(d_1) = u_2(d_1) = V_* \quad (3.6)$$

In this section we consider two problem, the first one is Couette flow, with zero pressure gradient. The second problem is Poiseuille flow for which the pressure gradient  $dp/dx$  is constant and equal to  $P$ .

Let us consider the first problem. The continuity equation (2.2) is automatically satisfied and from (2.7) – (2.12) we have

$$(\tau_{xz})_i = \mu_i \frac{\partial u_i}{\partial z} \quad (3.7)$$

$$(\tau_{yz})_i = (\tau_{yx})_i = 0 \quad (3.8)$$

$$(\sigma_x)_i = (\sigma_y)_i = (\sigma_z)_i = -p_i \quad (3.9)$$

the momentum equations (2.6),(2.7),(2.8) give;

$$\frac{\partial p_i}{\partial x} = \frac{\partial}{\partial z} \left( \mu_i \frac{\partial u_i}{\partial z} \right) \quad (3.10)$$

$$\frac{\partial p_i}{\partial y} = \frac{\partial p_i}{\partial z} = 0. \quad (3.11)$$

Equation (3.11) indicate that the pressure  $p$  is the independent of  $y$  and  $z$ . For the Couette flow we take  $p$  to be independent of  $x$  as well. This is the condition of zero pressure gradient. As a result of this assumption , equation (3.10) simplifies to

$$\frac{\partial}{\partial z} \left( \mu_i \frac{\partial u_i}{\partial z} \right) = 0. \quad (3.12)$$

Integrating (3.12), we obtain

$$u_1 = \frac{C_{11}}{\mu_1} z + C_{12} \quad (3.13)$$

$$u_2 = \frac{C_{21}}{\mu_2} z + C_{22} \quad (3.14)$$

where  $C_{11}, C_{12}$  are integration constants to be determined by boundary conditions.

Using boundary conditions (3.3), (3.4) and (3.6) we obtain

$$u_1 = \frac{V_*}{d_1} z \quad (3.15)$$

$$u_2 = V_* + (1 - V_*) \left( \frac{z - d_1}{1 - d_1} \right). \quad (3.16)$$

We find the  $V_*$  by using interface condition (3.5).

$$V_* = \frac{\mu_2 d_1}{\mu_1 d_2 + \mu_2 d_1} \quad (3.17)$$

We note that in the nondimensional variables used  $d_2 = 1 - d_1$

If we introduce  $m$ , and  $d$

$$m = \frac{\mu_1}{\mu_2}, \quad d = \frac{d_2}{d_1}, \quad (3.18)$$

then we have

$$V_* = \frac{1}{1 + md}, \quad (3.19)$$

$$u_1 = \frac{z/d_1}{1 + md}, \quad (3.20)$$

$$u_2 = \frac{1 + m((z/d_1) - 1)}{1 + md} \quad (3.21)$$

In the second problem, we consider the same plate geometry, same boundary conditions, and same interface conditions, but we consider a non zero pressure gradient given by

$$\frac{dp}{dx} = P. \quad (3.22)$$

The momentum equation now gives

$$\frac{\partial}{\partial z}(\mu_1 \frac{\partial u_1}{\partial z}) = P. \quad (3.23)$$

Integrating we have

$$u_1 = \frac{Pz^2}{2\mu_1} + \frac{C_{11}}{\mu_1}z + C_{12} \quad (3.24)$$

$$u_2 = \frac{Pz^2}{2\mu_2} + \frac{C_{21}}{\mu_2}z + C_{22}. \quad (3.25)$$

Using boundary conditions we obtain  $C_{11}$ ,  $C_{12}$ ,  $C_{21}$ ,  $C_{22}$  as

$$C_{11} = \frac{2V_*\mu_1 - Pd_1^2}{2d_1}, \quad C_{12} = 0 \quad (3.26)$$

$$C_{21} = \mu_2 \frac{V_* - 1}{d_1 - 1} - \frac{P}{2}(d_1 + 1), \quad (3.27)$$



$$C_{22} = \frac{d_1 - V_*}{d_1 - 1} + \frac{Pd_1}{2\mu_2} \quad (3.28)$$

from interface condition , we calculate the  $V_*$ ;

$$V_* = \frac{2\mu_2 - Pd_2}{2\mu_2(md + 1)} \quad (3.29)$$

additionally by substituting  $C_{11}$ ,  $C_{12}$ ,  $C_{21}$ ,  $C_{22}$  we obtain,

$$u_1 = \frac{Pd_1z}{2\mu_1} \left( \frac{z}{d_1} - 1 \right) + \frac{z}{d_1} V_* , \quad (3.30)$$

$$u_2 = \frac{P}{2\mu_2} \left( z^2 - z(d_1 + 1) + d_1 \right) + \frac{(V_* - 1)z - V_* + d_1}{d_1 - 1} \quad (3.31)$$

### 3b. Circular Cylinder

In this section we study the flow of two axial Newtonian fluids in a circular cylinder under the influence of a pressure gradient. We start our analysis with dimensional variables and we will later introduce a nondimensionalization which is slightly different from the one dimensionalization earlier.

Here we consider the fully developed flow of two superimposed Newtonian fluids in the circular cylinder by a radius  $R_1 + R_2$ . A cylindrical coordinate system  $(r, \theta, z)$  is used to describe the flow. The  $z$  axis coincides with the axis of the cylinder. one of the fluids occupies the inner region defined by

$$0 \leq r \leq R_1 \quad (3.32)$$

and the other fluid occupies the region defined by

$$R_1 \leq r \leq R_1 + R_2 \quad (3.33)$$

The fluids are immiscible, so that there is a sharp interface in the form of a cylindrical surface at  $r = R_1$ .

Because of the axial symmetry of the flow we have

$$u_z = U(r), \quad u_r = u_\theta = 0 \quad (3.34)$$

The interface velocity is again denoted by  $V_*$ , i.e.

$$U_1(R_1) = U_2(R_1) = V_* \quad (3.35)$$

The pressure gradient along the axis is constant and given by

$$\frac{\partial p}{\partial z} = P \quad (3.36)$$

We have one boundary condition at  $r = R_1 + R_2$  where the velocity must vanish. The momentum equations in cylindrical coordinate are (neglecting gravity)

$$\begin{aligned} \frac{\partial p}{\partial r} &= 0, \\ \frac{1}{r} \frac{\partial p}{\partial \theta} &= 0 \end{aligned} \quad (3.37)$$

$$\frac{\partial p}{\partial z} = P = \left( \frac{1}{r} \frac{\partial (r\tau_{rz})}{\partial r} \right) \quad (3.38)$$

The continuity equation is automatically satisfied. The normal and shear stresses are

$$(\tau_{rz})_i = \mu_i \frac{\partial U_i}{\partial r} \quad (3.39)$$

$$(\tau_{r\theta})_i = (\tau_{z\theta})_i = 0 \quad (3.40)$$

$$(\sigma_{rr})_i = (\sigma_{\theta\theta})_i = (\sigma_{zz})_i = -p_i \quad (3.41)$$

Index  $i=1$  denotes the inner flow while  $i=2$  denotes the outer flow. Substituting (3.39) in to (3.38) and integrating we obtain,

$$U_1(r) = \frac{r^2}{4\mu_1} P + \frac{C_{11}}{\mu_1} \ln|r| + C_{12} \quad (3.42)$$

$$U_2(r) = \frac{r^2}{4\mu_2} P + \frac{C_{21}}{\mu_2} \ln|r| + C_{22} \quad (3.43)$$

Using the condition that  $U_1$  must be finite at  $r = 0$ , we obtain  $C_{11} = 0$ . Using interface condition

$$U_1(R_1) = V_*,$$

we obtain  $C_{12}$  as

$$C_{12} = V_* - \frac{R_1^2}{4\mu_1} P \quad (3.44)$$

Similarly using  $U_2 = 0$  at  $r = R_1 + R_2$  we obtain

$$\frac{(R_1 + R_2)^2}{4\mu_2} P + \frac{C_{21}}{\mu_2} \ln|R_1 + R_2| + C_{22} = 0 \quad (3.45)$$

and using  $U_2(R_1) = V_*$  we obtain

$$V_* = \frac{R_1^2}{4\mu_2}P + \frac{C_{21}}{\mu_2}\ln|R_1| + C_{22}. \quad (3.46)$$

We can use equation (3.45) and (3.46) to solve for  $C_{21}$  and  $C_{22}$ . We obtain

$$C_{21} = \frac{\mu_2 V_* + \frac{P}{4}R_2(R_2 + 2R_1)}{\ln\left(\frac{R_1}{R_1 + R_2}\right)} \quad (3.47)$$

$$C_{22} = V_* - \frac{R_1^2}{4\mu_2}P - \frac{\ln R_1 (\mu_2 V_* + \frac{P}{4}R_2(R_2 + 2R_1))}{\mu_2 \ln\left(\frac{R_1}{R_1 + R_2}\right)} \quad (3.48)$$

$$U_1(r) = \frac{r^2}{4\mu_1}P + V_* - \frac{R_1^2}{4\mu_1}P \quad (3.49)$$

$$U_2(r) = V_* + \frac{(r^2 - R_1^2)}{4\mu_2}P - \left( \frac{V_* + \frac{P}{4\mu_2}R_2(R_2 + 2R_1)}{\ln\left(\frac{R_1 + R_2}{R_1}\right)} \right) \ln\left(\frac{r}{R_1}\right) \quad (3.50)$$

We nondimensionalize the variables by measuring velocities with respect to the interface velocity  $V_*$ ,  $P$  with respect to  $\frac{\mu_2 V_*}{(R_1 + R_2)^2}$ , and length with respect to  $R_1 + R_2$ . We introduce the parameter  $R = \frac{R_1}{R_1 + R_2}$ , which implies that for the inner region  $0 \leq r \leq R$  and for the outer region  $R \leq r \leq 1$ . We also introduce  $m = \mu_1/\mu_2$  and we have

$$U_1 = 1 + \frac{P}{4m}(r^2 - R^2) \quad (3.51)$$

$$U_2 = 1 + \frac{P}{4}(r^2 - R^2) - \left[ \frac{P}{4}(1 - R^2) + 1 \right] \left[ 1 - \frac{\ln r}{\ln R} \right]. \quad (3.52)$$

#### 4. SHEAR FLOW OF TWO UPPER CONVECTED MAXWELL FLUIDS

The results summarized in the previous chapter form the basis for discussion of the stability of stratified shear flows of immiscible multiple-component systems. The first investigation on the interfacial stability of two Newtonian viscous fluids in shearing motion was carried for plane Poiseuille/Couette flow by Yih[2]. Yih found that for these flows, viscosity stratification can cause an instability that persists even at vanishingly small Reynolds numbers. This low Reynolds-number instability is due to the presence of the fluid-fluid interface which introduces an "interfacial mode" of instability. Following Yih's work, similar linear-stability analyses have been performed for shear flows in different geometries for both Newtonian and viscoelastic fluids. A most comprehensive review on the subject is given in a monograph of Joseph and Renardy[3]. In this section we consider the zeroth order solution of plane Poiseuille/Couette flow of two superimposed viscoelastic fluids. The two fluids are assumed to obey the constitutive equation of the "Upper Convected Maxwell" (UCM) fluid. This analysis is partly based on the work of Renardy [4] who studied the stability of the interface in two-layer Couette flow of UCM liquids. The two fluids have different viscosities  $\mu_i$ , densities  $\rho_i$ , and relaxation times  $\lambda_i$ . Surface tension is assumed to exist at the interface.

The fluids are assumed to be immiscible. We consider the parallel plate geometry as discussed in chapter 3.

The lower fluid occupies the region defined by  $0 \leq z < d_1$  and the upper fluid occupies the region defined by  $d_1 \leq z < d_2$ . The index  $i = 1$  corresponds to the lower fluid and  $i = 2$  corresponds to the upper fluid.

The extra stress  $\underline{T}$  is given by equation (2.17) and since the problem is two dimensional with only x and z involved, we can simplify the stress matrix to

$$\underline{T} = \begin{bmatrix} \tau_{xx} & \tau_{xz} \\ \tau_{xz} & \tau_{zz} \end{bmatrix} \quad (4.1)$$

In this geometry the only non zero velocity  $u(z)$  is in the x direction and depends on z, hence

$$\underline{\nabla} u = \begin{pmatrix} 0 & \frac{\partial u}{\partial z} \\ 0 & 0 \end{pmatrix} \quad (4.2)$$

Considering that the flow is time independent and using (2.18) we have

$$\frac{D\underline{T}}{Dt} = - \begin{pmatrix} 2\tau_{xz} \frac{\partial u}{\partial z} & \tau_{zz} \frac{\partial u}{\partial z} \\ \tau_{zz} \frac{\partial u}{\partial z} & 0 \end{pmatrix} \quad (4.3)$$

Substituting this expression into (2.17) we obtain

$$\begin{bmatrix} \tau_{xx} & \tau_{xz} \\ \tau_{xz} & \tau_{zz} \end{bmatrix} + \lambda \begin{bmatrix} -2\tau_{xz} \frac{\partial u}{\partial z} & -\tau_{zz} \frac{\partial u}{\partial z} \\ -\tau_{zz} \frac{\partial u}{\partial z} & 0 \end{bmatrix} = \eta \begin{bmatrix} 0 & \frac{\partial u}{\partial z} \\ \frac{\partial u}{\partial z} & 0 \end{bmatrix} \quad (4.4)$$

or

$$\tau_{xx} - 2\lambda \tau_{xz} \frac{\partial u}{\partial z} = 0, \quad (4.5)$$

$$\tau_{xz} - \lambda \tau_{zz} \frac{\partial u}{\partial z} = \eta \frac{\partial u}{\partial z}, \quad (4.6)$$

$$\tau_{zz} = 0. \quad (4.7)$$

In view of (4.7) we can write (4.5) and (4.6) as

$$\tau_{xx} = 2 \lambda \eta \left( \frac{\partial u}{\partial z} \right)^2, \quad (4.8)$$

$$\tau_{xz} = \eta \frac{\partial u}{\partial z}, \quad (4.9)$$

using equation (2.16) we have

$$\underline{S} = \begin{bmatrix} -p + \tau_{xx} & \tau_{xz} \\ \tau_{xx} & 0 \end{bmatrix}, \quad (4.10)$$

where the pressure  $p$  is a function of  $x$  only. From the momentum equation in the  $x$ -direction we obtain

$$-\frac{\partial p}{\partial x} + \frac{\partial \tau_{xz}}{\partial z} = 0 \quad (4.11)$$

For the Couette flow between two parallel plates  $\frac{\partial p}{\partial x} = 0$ , hence we have

$$\frac{\partial \tau_{xz}}{\partial z} = 0. \quad (4.12)$$

If we substitute  $\tau_{xz}$  from (4.9) we have

$$\frac{\partial}{\partial z} \left( \eta \frac{\partial u}{\partial z} \right) = 0 \quad (4.13)$$

Integrating the equation we obtain

$$u_i = \frac{a_i}{\eta_i} z + b_i \quad i = 1, 2 \quad (4.14)$$

and we write for each  $i$  index,

$$u_1 = \frac{a_1}{\eta_1} z + b_1, \quad (4.15)$$

$$u_2 = \frac{a_2}{\eta_2} z + b_2. \quad (4.16)$$

Here  $a_1, a_2, b_1, b_2$  are constants to be determined by applying boundary conditions.

Boundary Conditions are

$$\begin{aligned} u_1(0) &= 0, \\ u_2(1) &= 1 \end{aligned} \quad (4.17)$$

and interface conditions are

$$\begin{aligned} -(\tau_{xz})_1 &= -(\tau_{xz})_2, \\ u_1(d_1) &= u_2(d_1) = V_* \end{aligned} \quad (4.18)$$

where  $V_*$  is the velocity at the interface.

We consequently obtain,

$$u_1 = \frac{V_*}{d_1} z \quad (4.19)$$

$$u_2 = \frac{1 - V_*}{1 - d_1} z + \frac{V_* - d_1}{1 - d_1} \quad (4.20)$$

to find  $V_*$  we apply the interface condition, then we have

$$V_* = \frac{1}{1 + nd} \quad (4.21)$$

where the quantities  $n$ , and  $d$  are defined as

$$n = \frac{\eta_1}{\eta_2}, d = \frac{d_2}{d_1}. \quad (4.22)$$



We now consider the more general problem where the upper plate moves with a constant velocity, the lower plate is stationary and there is a pressure gradient  $P$  in the x-direction. For this case the momentum equation gives (4.11) gives

$$\frac{\partial \tau_{xz}}{\partial z} = P \quad (4.23)$$

Substituting (4.9) into (4.23) we have

Here, first we substitute  $c_2$  into (4.18)

$$P = \frac{\partial}{\partial z} \left( \eta \frac{\partial u}{\partial z} \right), \quad (4.24)$$

for each of the layers.

Integrating we obtain,

$$u_1 = \frac{Pz^2}{2\eta_1} + \frac{c_{11}}{\eta_1}z + c_{12} \quad (4.25)$$

$$u_2 = \frac{Pz^2}{2\eta_2} + \frac{c_{21}}{\eta_2}z + c_{22} \quad (4.26)$$

We apply the boundary conditions (4.17) and (4.18) to obtain  $c_{11}$ ,  $c_{12}$ ,  $c_{21}$ ,  $c_{22}$ .

These are given by

$$c_{11} = \frac{2V_*\eta_1 - Pd_1^2}{2d_1}, \quad c_{12} = 0, \quad (4.27)$$

$$c_{21} = \frac{V_* - 1}{d_1 - 1}\eta_2 - \frac{P}{2}(d_1 + 1) \quad (4.28)$$

$$c_{22} = 1 + \frac{Pd_1}{2\eta_2} - \frac{V_* - 1}{d_1 - 1} \quad (4.29)$$

by using interface condition  $V_*$  is obtained.

$$V_* = \frac{2\eta_2 - Pd_2}{2\eta_2(1 + nd)} \quad (4.30)$$

and by substituting  $c_{11}$ ,  $c_{12}$ ,  $c_{21}$ ,  $c_{22}$

$$u_1 = \frac{Pz^2}{2\eta_1} + \frac{2V_*\eta_1 - Pd_1^2}{2d_1\eta_1}z \quad (4.31)$$

$$u_2 = \frac{Pz^2}{2\eta_2} + \left( \frac{V_* - 1}{d_1 - 1} - \frac{P}{2\eta_2}(d_1 + 1) \right)z + 1 + \frac{Pd_1}{2\eta_2} - \frac{V_* - 1}{d_1 - 1} \quad (4.32)$$

## 5. FLOW OF TWO GIESEKUS TYPE VISCOELASTIC FLUIDS

The problem that we discuss in this chapter is a Couette flow of two incompressible viscoelastic liquids obeying the Giesekus one-mode "linear" model. We have in view primarily flows of dilute polymer solutions or concentrated polymer solutions and melts of flexible polymer molecules which are the two important classes of viscoelastic fluids.

Both dilute solutions and melts have first normal stress differences of significant magnitude. However the shear viscosity of concentrated solutions and melts decreases by three orders of magnitude as shear rate increases. But similar case dilute solutions have little shear thinning. In concentrated solutions and melts the first normal stress coefficient,  $\psi_1 = N_1/\chi^2$  can decrease by several orders of magnitude as  $\chi$  increases. This decrease in  $\psi_1$  is another manifestation of shear thinning. In addition concentrated solutions have a significant negative second normal stress coefficient  $\psi_2 = N_2/\chi^2$ . In dilute solutions this quantity is almost zero. Both shear thinning and a non zero second normal stress differences are predicted to play major roles in controlling stability in viscoelastic flows. The stability characteristics of dilute solutions are completely different from those of melts. [5]

The behavior of these fluids can be modeled by the Giesekus type viscoelastic fluid. The constitutive equation for this fluid was introduced in chapter 2 (cf. equation (2.21)-(2.24)). We consider again the two parallel plates geometry with a planar interface separate two immiscible fluids. The distance between the plates is taken

equal to 1, the lower fluid occupies the region  $0 \leq z \leq d_1$  while the upper fluid occupies the region defined by  $d_1 \leq z \leq d_2$ .

The extra viscoelastic stress contribution  $\underline{T}$  which is introduced by equation (2.21) has the form.

$$\underline{T} = \begin{bmatrix} \tau_{xx} & 0 & \tau_{xz} \\ 0 & \tau_{yy} & 0 \\ \tau_{xz} & 0 & \tau_{zz} \end{bmatrix} \quad (5.1)$$

This form of the stress tensor is implied by the fact that there is no velocity in the y direction and the non zero velocity  $u(z)$  is in the x direction and depends only on z.

We consequently have

$$\underline{\nabla} \underline{u} = \begin{pmatrix} 0 & 0 & \frac{\partial u}{\partial z} \\ 0 & 0 & 0 \\ 0 & 0 & 0 \end{pmatrix} \quad (5.2)$$

Considering that the problem is time independent we use equation (2.18) to obtain

$\frac{DT}{Dt}$ . We have

$$\frac{DT}{Dt} = - \begin{bmatrix} 2 \frac{\partial u}{\partial z} \tau_{xz} & 0 & \frac{\partial u}{\partial z} \tau_{zz} \\ 0 & 0 & 0 \\ \frac{\partial u}{\partial z} \tau_{zz} & 0 & 0 \end{bmatrix}. \quad (5.3)$$

We substitute (5.3) into (2.36) and we obtain

$$\begin{aligned}
& \begin{bmatrix} \tau_{xx} & 0 & \tau_{xz} \\ 0 & \tau_{yy} & 0 \\ \tau_{xz} & 0 & \tau_{zz} \end{bmatrix} - W_e \begin{bmatrix} 2\frac{\partial u}{\partial z}\tau_{xz} & 0 & \frac{\partial u}{\partial z}\tau_{zz} \\ 0 & 0 & 0 \\ \frac{\partial u}{\partial z}\tau_{zz} & 0 & 0 \end{bmatrix} \\
& + \frac{\alpha W_e}{\eta} \begin{bmatrix} (\tau_{xx})^2 + (\tau_{xz})^2 & 0 & \tau_{xx}(\tau_{xx} + \tau_{zz}) \\ 0 & (\tau_{yy})^2 & 0 \\ (\tau_{xz})(\tau_{xx} + \tau_{zz}) & 0 & (\tau_{xz})^2 + (\tau_{zz})^2 \end{bmatrix} = \eta \begin{bmatrix} 0 & 0 & \frac{\partial u}{\partial z} \\ 0 & 0 & 0 \\ \frac{\partial u}{\partial z} & 0 & 0 \end{bmatrix}. \quad (5.4)
\end{aligned}$$

We have four scalar equations from the above matrix equation. These are

$$\tau_{xx} - 2W_e \frac{\partial u}{\partial z} \tau_{xz} + \frac{\alpha W_e}{\eta} ((\tau_{xx})^2 + (\tau_{xz})^2) = 0, \quad (5.5)$$

$$\tau_{xz} - W_e \frac{\partial u}{\partial z} \tau_{zz} + \frac{\alpha W_e}{\eta} \tau_{xz} (\tau_{xx} + \tau_{zz}) = \eta \frac{\partial u}{\partial z}, \quad (5.6)$$

$$\tau_{yy} + \frac{\alpha W_e}{\eta} (\tau_{yy})^2 = 0, \quad (5.7)$$

$$\tau_{zz} + \frac{\alpha W_e}{\eta} (\tau_{xz}^2 + \tau_{zz}^2) = 0, \quad (5.8)$$

If we introduce the Weissenberg number  $W_e$  which appears in these equation is the nondimensional relaxation time  $\bar{\lambda}$  is given by (2.27). We introduce  $\beta$ , and  $\chi$  by

$$\beta = \frac{W_e}{\eta}, \quad (5.9)$$

$$\chi = \eta \frac{\partial u}{\partial z}. \quad (5.10)$$

We can write

$$\tau_{xx} - 2\beta\chi\tau_{xz} + \alpha\beta(\tau_{xx}^2 + \tau_{xz}^2) = 0, \quad (5.11)$$

$$\tau_{xz} - \beta\chi\tau_{zz} + \alpha\beta\tau_{xz}(\tau_{xx} + \tau_{zz}) = \chi, \quad (5.12)$$

$$\tau_{yy} + \alpha\beta(\tau_{yy})^2 = 0, \quad (5.13)$$

$$\tau_{zz} + \alpha\beta(\tau_{xz}^2 + \tau_{zz}^2) = 0. \quad (5.14)$$

From equation (5.13)

$$\tau_{yy} = 0. \quad (5.15)$$

We introduce the first normal stress difference

$$N_1 = \tau_{xx} - \tau_{zz}, \quad (5.16)$$

and the second normal stress difference

$$N_2 = \tau_{yy} - \tau_{zz}. \quad (5.17)$$

We use  $\tau$  to denote the shear stress  $\tau_{xz}$  and we note that the Newtonian shear stress is given by

$$\tau^s = \tau_{xz}^s = \frac{\mu}{\eta}\chi \quad (5.18)$$

where  $\chi$  is the shear rate given by (5.10).

From (5.15) and (5.17) we have,

$$N_2 = -\tau_{zz}, \quad (5.19)$$

$$N_1 - N_2 = \tau_{xx}. \quad (5.20)$$

Substituting (5.19) and (5.20) into equations (5.11), (5.12), (5.14),

$$N_1 - N_2 - 2\beta\tau\chi + \alpha\beta[(N_1 - N_2)^2 + \tau^2] = 0, \quad (5.21)$$

$$\tau + \beta\chi N_2 + \alpha\beta\tau(N_1 - 2N_2) = \chi, \quad (5.22)$$

$$-N_2 + \alpha\beta(\tau^2 + N_2^2) = 0. \quad (5.23)$$

Subtracting (5.23) from (5.21) we write

$$N_1\{1 + \alpha\beta(N_1 - 2N_2)\} = 2\beta\tau\chi. \quad (5.24)$$

Equation (5.22) can be written as

$$\tau\{1 + \alpha\beta(N_1 - 2N_2)\} = \chi(1 - \beta N_2), \quad (5.25)$$

and from (5.23)

$$N_2(1 - \alpha\beta N_2) = \alpha\beta\tau^2. \quad (5.26)$$

From (5.24) and (5.25) we write

$$\tau^2 = N_1 \frac{(1 - \beta N_2)}{2\beta}. \quad (5.27)$$

Using (5.27) in (5.26)

$$N_1 = \frac{2N_2(1 - \alpha\beta N_2)}{(1 - \beta N_2)}. \quad (5.28)$$

Equations (5.28), (5.27), (5.25) provide the expressions required in the evaluation of  $N_1$ ,  $\tau$ ,  $\chi$  in terms of a given value of  $N_2$ . In order to allow the calculation of the stresses  $N_1$ ,  $N_2$ , and  $\tau$  in terms of the deformation gradient  $\chi$  we need to introduce a variable  $\Lambda$  by the equation

$$\beta N_2 = \frac{1 - \Lambda}{1 + (1 - 2\alpha)\Lambda}. \quad (5.29)$$

In terms of  $\Lambda$  we can solve (5.28) to obtain

$$N_1 = \frac{1 - \Lambda^2}{\alpha\beta\Lambda(1 + (1 - 2\alpha)\Lambda)}. \quad (5.30)$$

Using (5.28) and (5.29) into (5.25) we obtain

$$\tau = \frac{2(1 - \alpha)\Lambda^2}{1 + (1 - 2\alpha)\Lambda}\chi. \quad (5.31)$$

From (5.25) and (5.27) we can obtain

$$\chi^2 = \frac{N_1\{1 + \alpha\beta(N_1 - 2N_2)\}}{2\beta(1 - \beta N_2)}, \quad (5.32)$$

we can then use (5.29) and (5.30) to obtain

$$\chi^2 = \frac{1 - \Lambda^2}{4\alpha\beta^2\Lambda^4(1 - \alpha)}. \quad (5.33)$$

We can now see the advantage of the transformation (5.29). Equation (5.32) provides a quadratic relations for the solution of  $\Lambda^2$  in terms of  $\chi$ . We can explicitly calculate  $\tau$  from (5.31)  $N_1$  from (5.30) and  $N_2$  from (5.29).

This general formulation is valid for non zero values of the parameters  $\alpha$ ,  $\beta$ ,  $\eta$ .

---

Now, we will consider some special cases.

a-)  $\beta = \eta = 0$

from (5.10) and (5.21)- (5.23)

$$N_1 = N_2 = \tau = \chi = 0$$

This is the Newtonian case that we studied in chapter three.

b-)  $\alpha = 0 ; (\beta \neq 0)$

in this case we have  $N_1 = 2\beta\tau\chi$ ,  $N_2 = 0$  and  $\tau = \chi$  (5.34)

This is the Oldroyd B type fluid . Notice that if the solvent term in the Oldroyd B equation is set to zero that is  $\mu=0$  the equation reduces the UCM equations.

Here both the upper-convected Maxwell and the Oldroyd B models show a zero second normal difference  $N_2$  and no shear thinning. These might be acceptable approximations for dilute solutions but are poor approximations for melts. Also there are some important limitations of the Oldroyd B equations for describing dilute solutions are :



The model contains only a single relaxation time, while the fluid actually displays a spectrum of time constants, and extensional viscosities grows limitless, in extensional flows when the extensional strain rate exceeds a critical value.

From the momentum equation in the x-direction we obtain

$$-\frac{\partial p}{\partial x} + \frac{\partial S_{xz}}{\partial z} = 0 \quad (5.35)$$

where the stress tensor  $\underline{S}$  is defined by equation (2.21).

For the Couette flow between two parallel plates  $\frac{\partial p}{\partial x} = 0$ , hence we have

$$\frac{\partial S_{xz}}{\partial z} = 0. \quad (5.36)$$

From the equation (2.21) we have

$$S_{xz} = \tau_{xz}^s + \tau, \quad (5.37)$$

where  $\tau$  denotes the extra shear stress  $\tau_{xz}$ .

Substituting (5.18) and (5.31) into (5.37) we obtain

$$\tau_{xz} = \left( \frac{\mu}{\eta} + \frac{2(1-\alpha)\Lambda^2}{1+(1-2\alpha)\Lambda} \right) \chi. \quad (5.38)$$

Equation (5.36) implies that  $S_{xz}$  must be constant. In view of (5.38) and (5.33) we conclude that  $\chi$  must be a constant. Consequently we can integrate equation (5.10) for the upper and lower fluid to obtain

$$u_1 = \frac{\chi_1}{\eta_1} z + c_{11}, \quad (5.39)$$

$$u_2 = \frac{\chi_2}{\eta_2} z + c_{12}. \quad (5.40)$$

From the boundary condition at  $u_1 = 0$  at  $z = 0$ , we obtain  $c_{11} = 0$ . From the boundary condition  $u_2 = 1$  for  $z = 1$  we obtain

$$c_{12} = 1 - \frac{\chi_2}{\eta_2}. \quad (5.41)$$

We denote by  $V_*$  the velocity at the interface  $z = d_1$ . From (5.39) and (5.40) we see that

$$V_* = \frac{\chi_1 d_1}{\eta_1} = \frac{\chi_2 d_1}{\eta_2} + 1 - \frac{\chi_2}{\eta_2} \quad (5.42)$$

The interface stress condition can be written as,

$$\mu_1 \frac{\chi_1}{\eta_1} + \frac{2(1 - \alpha_1)\Lambda_1^2 \chi_1}{1 + (1 - 2\alpha_1)\Lambda_1} = \mu_2 \frac{\chi_2}{\eta_2} + \frac{2(1 - \alpha_2)\Lambda_2^2 \chi_2}{1 + (1 - 2\alpha_2)\Lambda_2}. \quad (5.43)$$

Using (5.42) we can write

$$\frac{\chi_1}{\eta_1} = \frac{V_*}{d_1}, \quad \frac{\chi_2}{\eta_2} = \frac{U - V_*}{d_2} \quad (5.44)$$

If we replace  $\chi_1$ , and  $\chi_2$  in (5.43) by their expression (5.44) we obtain an equation for  $V_*$  of the form ,

$$\mu_1 \frac{V_*}{d_1} + \frac{2\eta_1(1 - \alpha_1)\Lambda_1^2 V_*}{d_1[1 + (1 - 2\alpha_1)\Lambda_1]} = \mu_2 \frac{(1 - V_*)}{d_2} + \frac{2\eta_2(1 - \alpha_2)\Lambda_2^2(1 - V_*)}{d_2[1 + (1 - 2\alpha_2)\Lambda_2]} \quad (5.45)$$

Here  $\Lambda_1, \Lambda_2$  are given , in view of equation (5.33) , by

$$\frac{V_*^2}{d_1^2} = \frac{1 - \Lambda_1^2}{4\alpha_1\beta_1^2\eta_1^2\Lambda_1^4(1 - \alpha_1)}, \quad (5.46)$$

$$\frac{(1 - V_*)^2}{d_2^2} = \frac{1 - \Lambda_2^2}{4\alpha_2\beta_2^2\eta_2^2\Lambda_2^4(1 - \alpha_2)}. \quad (5.47)$$

Equation (5.41) and (5.42) can be solved analytically for  $\Lambda_1, \Lambda_2$  in terms of  $V_*$ . For this we call

$$A = \frac{4\alpha_1\beta_1^2\eta_1^2(1 - \alpha_1)}{d_1^2}, \quad (5.48)$$

and (5.46) becomes

$$AV_*^2\Lambda_1^4 + \Lambda_1^2 - 1 = 0. \quad (5.49)$$

Solving for

$$Y_1 = \Lambda_1^2 \quad (5.50)$$

we obtain

$$\Lambda_1^2 = \frac{-1 + \sqrt{1 + 4AV_*^2}}{2AV_*^2}. \quad (5.51)$$

Similarly, for equation (5.47) we define B as

$$B = \frac{4\alpha_2\beta_2^2\eta_2^2(1 - \alpha_2)}{d_2^2} \quad (5.52)$$

and we obtain  $\Lambda_2^2$  as,

$$\Lambda_2^2 = \frac{-1 + \sqrt{(1 + 4B(1 - V_*)^2)}}{2B(1 - V_*)^2}. \quad (5.53)$$

We can now establish an iterative procedure for solving equation (5.45) for  $V_*$ . We start with the choice  $V_* = d_1$  (which corresponds to the single fluid flow) and use (5.51) and (5.53) to calculate  $\Lambda_1$  and  $\Lambda_2$  we can then proceed evaluating the residual of equation (5.45). A root finding technique can then be utilized to improve the estimate of  $V_*$ . Having obtained  $V_*$  we can use (5.42) to calculate  $\chi_1$ , and  $\chi_2$  and (5.51) and (5.53) to calculate  $\Lambda_1$  and  $\Lambda_2$ . We can then obtain the normal stress difference  $N_1$ ,  $N_2$  and the shearing stress  $\tau$  using equations (5.29)- (5.31).

The procedure described above has been used to produce the data illustrated in figures 4-39. The various cases considered are summarized in table 1. In all cases the Newtonian viscosities  $\mu_1, \mu_2$  are chosen to be equal zero. This is done in order to emphasize the viscoelastic character of the fluid. We note that several stability studies have shown an important stabilizing effect of the Newtonian viscosities. The strategy used here to illustrate the results of these calculations is the following: The network viscosity  $\eta_1$  of the fluid in the lower layer is kept equal to 1 (i.e. viscosities are normalized with respect to the network viscosity of the lower layer). Similarly the Weissenberg number  $We_1$  of the fluid in lower layer is kept equal to 1 (this implies that the relaxation time of the fluid in the lower layer is equal to  $d_{ref}/U_{ref}$ . Here  $d_{ref}$  is the distance between the plates  $U_{ref}$  is the velocity of the upper plate). The velocity gradients in both the lower and upper layer and the corresponding shear and normal stress differences are plotted as functions of the network viscosity of the upper layer. This is done for values of the mobility parameters  $\alpha_i$  varying between 0.1 and 0.5. We only consider cases for which the mobility parameters of the upper and lower fluids are equal.

We consider three different values (1, 0.2, 2) for the Weissenberg number of the fluid in the upper layer. For each one of these cases we consider three different layer configurations. In the first configuration the layers are equal of depth. Then we consider a this layer in the bottom (near the stationary plate) at ratio 1:9 and consequently consider a this layer near the top plate (which moves) again at ratio 1:9. The letters A,B,...I are used to name the nine cases described above (see table 1). Figures 4a and 4b depict the velocity gradient  $\chi_1, \chi_2$  which are related to the actual velocity gradients  $\frac{du}{dz}$  by relation (5.10). Consequently  $\chi_1$  is indeed the velocity gradient, but  $\chi_2$  is equal to the product of  $\eta_2$  with the velocity gradient of the fluid in the upper layer.

We observe that all curves of figure 4a as well as all curves of figure 4b pass through the point  $\eta_2 = 1, \chi_1 = \chi_2 = 1$ . This, of course, is an expected result since for this case A and for  $\eta_2 = 1$  we have a configuration consisting of a single fluid. For a single fluid the velocity gradient is equal to 1 due to the normalization utilized in this thesis. Figures 4a, 4b also show that increasing values of the mobility parameters  $\alpha_i$  in the case of a less viscous top layer result in a decrease in the velocity gradient  $\chi_1$  with a corresponding increase in  $\chi_2$ . The fact that a decrease in  $\chi_1$  must be accompanied by an increase in  $\chi_2$  can be explained by the consideration of the velocity  $V_*$  at the interface (see figure 3). A decrease in  $V_*$  results in a decrease in  $\chi_1$  and an increase in  $\chi_2$  while the reverse happens for an increase of  $V_*$ .

Figure 5 illustrates the variation of the shearing stress  $\tau$  with the viscosity of the top layer, for various values of the mobility parameter. In all of the cases studied here the shearing stress  $\tau$  is the total shearing stress in the fluid, since the Newtonian viscosities are taken equal to zero. In the Couette flow considered here the shearing

stress remains constant throughout the layer. Consequently the continuity of the shearing stress condition at the interface implies that  $\tau_1 = \tau_2$ . We also note that for  $\eta_2=1$  (case of a single fluid with velocity gradient 1),  $\tau_1 \neq 1$ . this is, of course, due to the nonlinear character of the fluid due to the non zero values of the mobility parameter.

Figures 6a and 6b depict the first normal stress differences  $N_{11}$  and  $N_{12}$  as function of the upper layer viscosity  $\eta_2$ . We note the maximum reached by the first normal stress differences in the upper layer. Similar results for the second normal stress differences are depicted in figures 7a and 7b. In view of equation (5.34) we note that when  $\eta_2 = 1$ , and  $\alpha \rightarrow 0$  the first normal stress differences should tend to 2 while the second normal stress differences should tend to zero. Figures 6 and 7 clearly indicate these tendencies.

Figures 8 to 11 illustrate the variation of the velocity gradients  $\chi_1, \chi_2$  the shearing stress differences  $N_1$  and  $N_2$  with the viscosity of the upper layer  $\eta_2$ , for the case B of table 1. Case B differs from case A because of the Weissenberg number of the upper fluid is much lower. The differences observed between cases A and B are;

a) Velocity gradient in the lower layer increases for increasing values of the mobility parameter. This is opposite of what is observed in the case of equal Weissenberg numbers when the lower layer is more viscous than the upper layer.

b) The first normal stress differences in the upper layer tend to 0.4 as  $\alpha \rightarrow 0$  and  $\eta_2 = 1$ . The first normal stress differences in the lower layer still tend to 2 for  $\alpha \rightarrow 0$  and  $\eta_2 = 1$ . This is explained by equation (5.33) which predicts that in this limit

$$N_1 \sim 2\beta$$

c) The second normal stress differences should tend to zero as  $\alpha \rightarrow 0$  however in the upper layer they are significantly lower than the common stress of case A. Figures 12- 15 depict the corresponding graphs for case C of table 1. Here the Weissenberg number for the upper layer is taken to be equal to 2. The graphs for this case are similar to the ones obtain for case A with the exemption that there is no common point of the velocity gradient curves for  $\eta_2 = 1$  as is the case in A. The fact that case C differs from A less than B does from A is of course explained by the fact that  $We_2$  in C is twice as large while in B is 1/5 of its value in case A.

Figures 16- 19 depict the velocity gradients, shear stress, and normal stress differences for the case D of table 1. Here we consider a thin layer of fluid near the bottom stationary plate. The Weissenberg numbers of both fluids are equal to 1. When the viscosity of the upper layer is less than the viscosity of the lower layer then  $\chi_2$  remains very close to 1 for all values of the mobility parameters  $\alpha$ . The behavior of the shearing and normal stress differences for this case is similar to the case A.

Figures 20-23 depict the corresponding for case E of the table 1. The difference between E and D is essentially the reduction of the second normal stress difference in the upper layer due to the lesser value of  $We_2$ . In addition we note that the influence of the mobility parameter on the velocity gradient, shearing stress and first normal stress difference of the upper layer is reduced.

The corresponding result for the case F of table 1 are given in figures 24-27.

Figures 28-31 depict again the velocity gradients, shear stress, and normal stress differences as function of the network viscosity of the upper layer for the case G of table 1. Figure 29-32 depict similar graph for the case H for which the Weissenberg number of the upper fluid is 115 of the  $We$  number of the lower fluid.

A common characteristic of all these curves appears to occur for  $\eta_2/\eta_1 > 1$ . This is the case of a thin highly viscous layer between the lower fluid and the moving upper plate. For this configurations the velocity gradients, the shear stress and the normal stress differences seem to depend weakly on the network viscosity. Their values are strongly influenced by the values of the mobility parameter  $\alpha$ .

Case I of table 1 is depicted in figures 36-39.



## 6. CONCLUSIONS

The steady state solution of shear flows associated with multiple-layered fluids can easily be obtained in a variety of fluid configurations. For the geometry of two parallel plates and a circular cylinder, closed form analytic solutions are available when we have two superimposed newtonian fluids or two viscoelastic fluids characterized by the UCM model.

For the Giesekus model used in this thesis which is capable of predicting second normal stress differences and shear thinning, we use an accurate and simple numerical solution approach. As expected, the second normal stress difference increases for increasing values of the mobility parameter  $\alpha$ . In addition, increased Weissenberg numbers produce higher second normal stress differences.

In the cases where one of the layers is much thinner than the other, we conclude that the nondimensional velocity gradient in the thick layer remains very close to 1 for all values of the mobility parameter, provided that its viscosity is less than that of the thin layer. This result is more pronounced when the Weissenberg numbers of both fluids are nearly equal.

Again, in the cases where the layer next to the moving plate is much thinner than the other, we conclude that the velocity gradient and the normal stress differences exhibit a pronounced maximum for a specific ratio of the network viscosities. The amplitude of the maximum increases for larger values of the mobility parameters .

we d	We <sub>1</sub> = 1, We <sub>2</sub> = 1	We <sub>1</sub> = 1, We <sub>2</sub> = 0.2	We <sub>1</sub> = 1, We <sub>2</sub> = 2
d <sub>1</sub> =d <sub>2</sub> =0.5	A	B	C
d <sub>1</sub> = 0.1 d <sub>2</sub> = 0.9	D	E	F
d <sub>1</sub> = 0.9 d <sub>2</sub> = 0.1	G	H	I

*TABLE 1.* Summary of flow characteristics of the examples studied

$\mu_1 = \mu_2 = 0$ ,  $\eta_1 = 1$ ,  $\chi(i)$ ,  $N_1(i)$ ,  $N_2(i)$ ,  $\tau$ , versus  $\eta_2$

for  $\alpha_1 = \alpha_2 = 0.1, 0.2, 0.3, 0.4, 0.5$ .

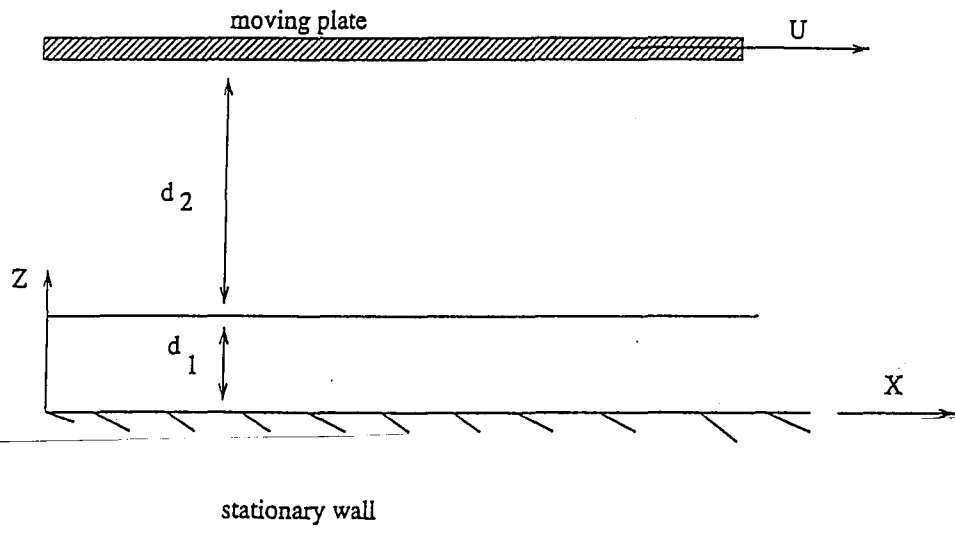


FIGURE 1. The parallel plates geometry.

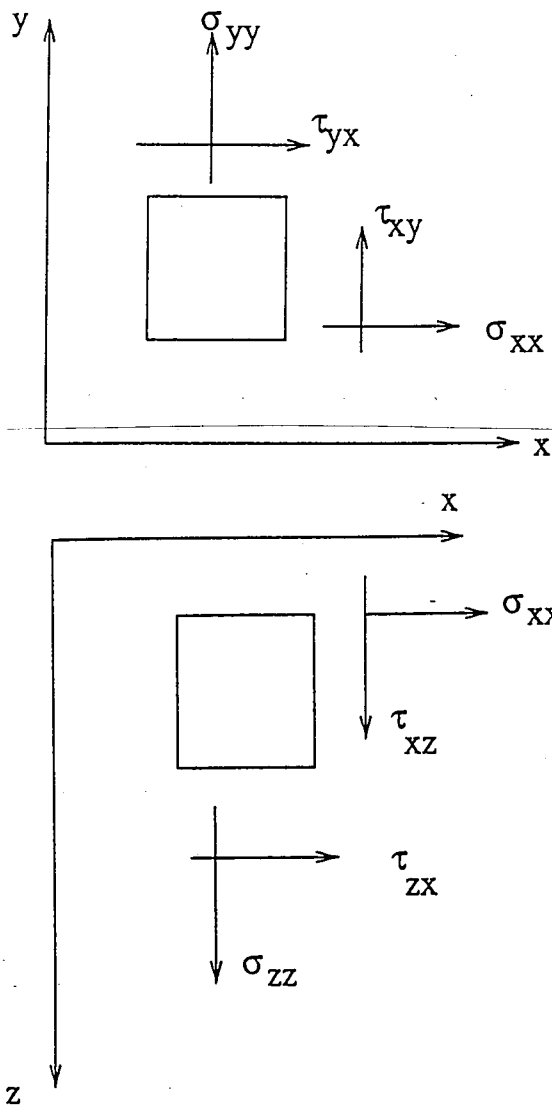


FIGURE 2. The components of the stress tensor  $\underline{S}$

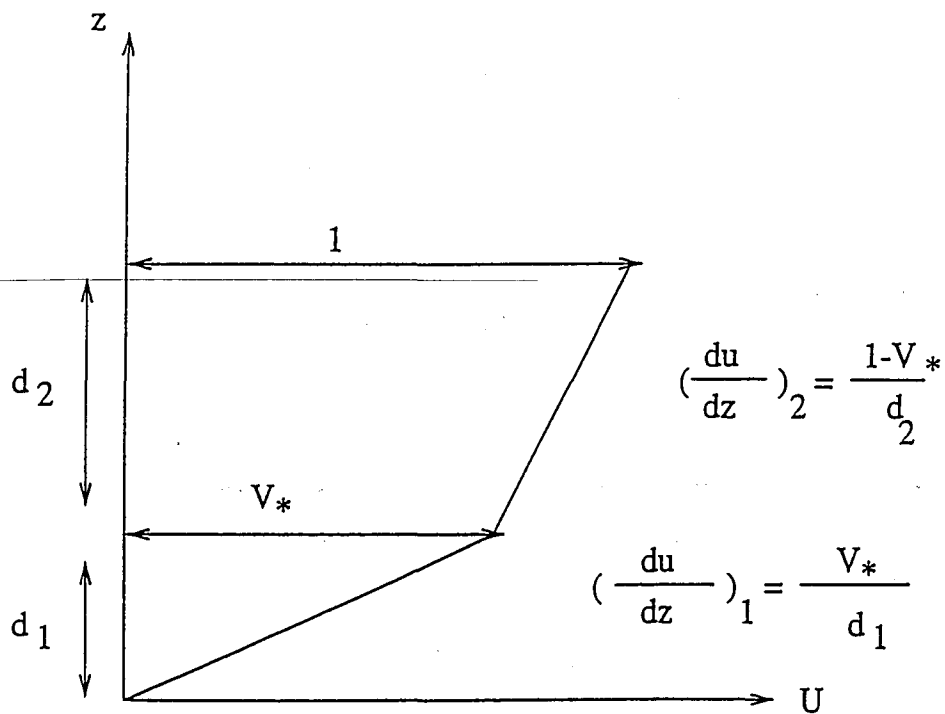
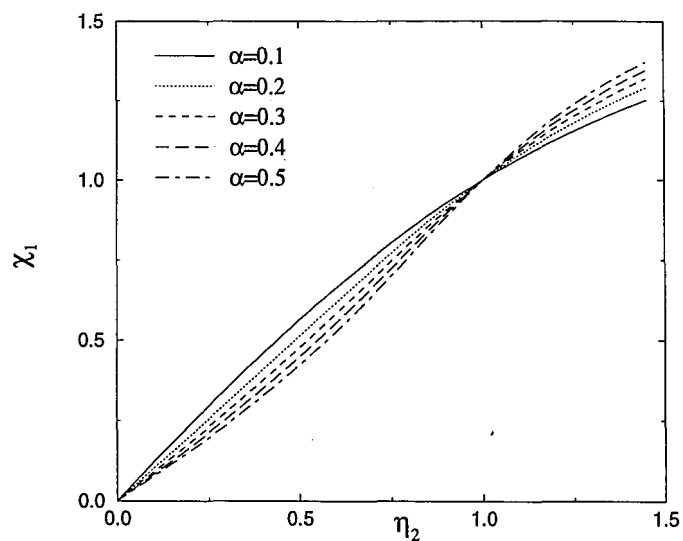
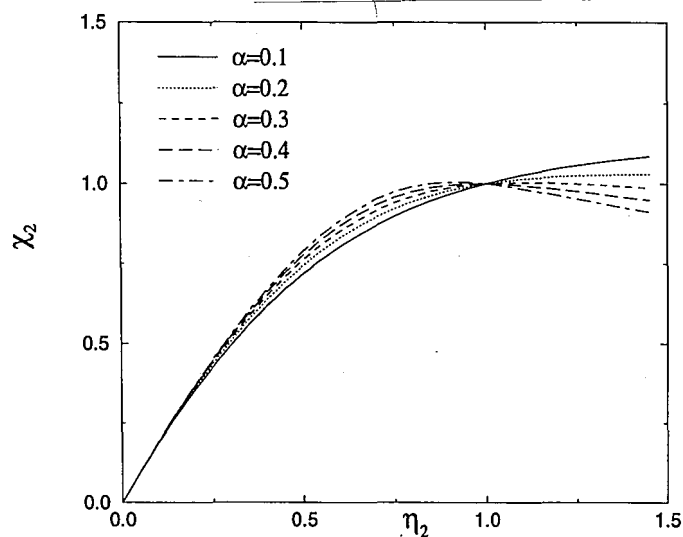


FIGURE 3. The relation between  $V_*$  and the velocity gradient.



(4a)



(4b)

FIGURE 4. The velocity gradients  $\chi_i$  in the two layers as functions of the network viscosity  $\eta$  of the upper layer for values of the network mobility parameter  $\alpha$  between 0.1 and 0.5. Case A where  $We_1 = We_2 = 1$ ,  $d_1 = d_2 = 0.5$ . The Newtonian viscosity are zero, the network viscosity of the lower layer is fixed at 1. a)  $\chi_1$  vs.  $\eta_2$  b)  $\chi_2$  vs.  $\eta_2$

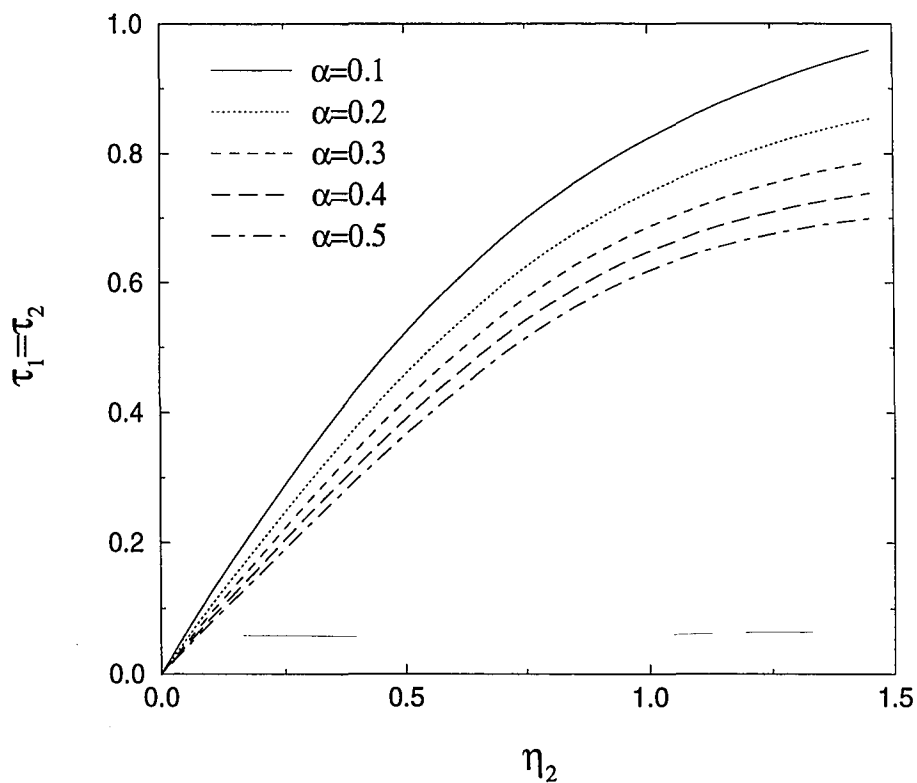
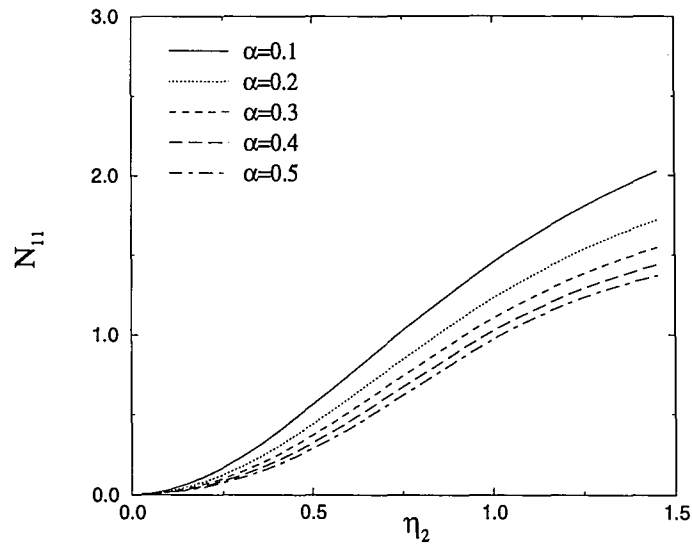
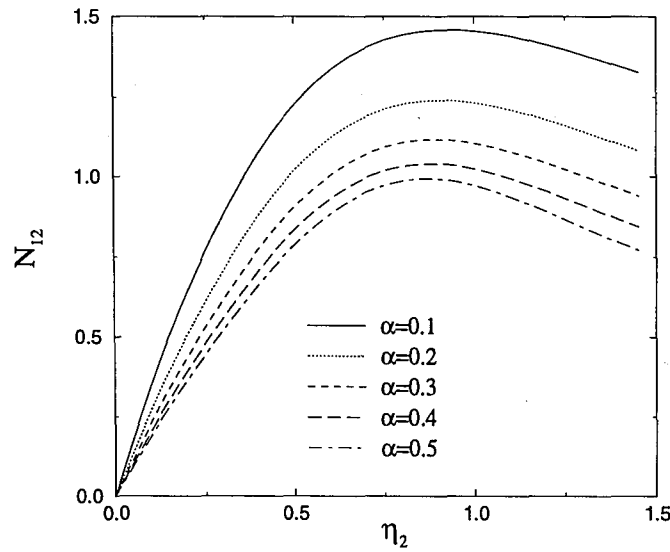


*FIGURE 5.* The shear stress  $\tau_i$  in the two layers as functions of the network viscosity  $\eta$  of the upper layer for values of the network mobility parameter  $\alpha$  between 0.1 and 0.5. Case A where  $We_1 = We_2 = 1$ ,  $d_1 = d_2 = 0.5$ . The Newtonian viscosity are zero, the network viscosity of the lower layer is fixed at 1.



(6a)

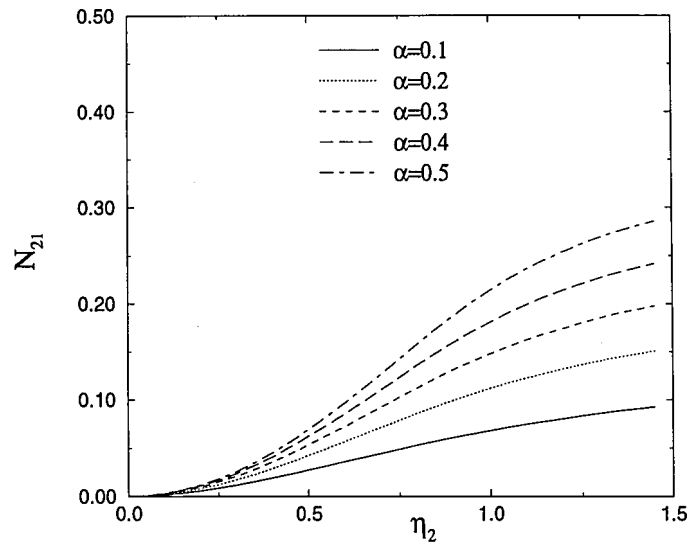


(6b)

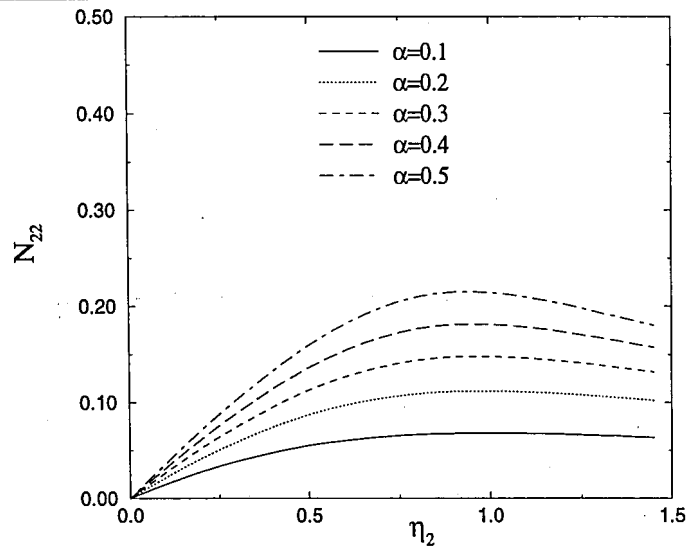
**FIGURE 6.** The first normal stress  $n_{1i}$  in the two layers as functions of the network viscosity  $\eta$  of the upper layer for values of the network mobility parameter  $\alpha$  between 0.1 and 0.5. Case A where  $We_1 = We_2 = 1$ ,  $d_1 = d_2 = 0.5$ . The Newtonian viscosity are zero, the network viscosity of the lower layer is fixed at 1.

a)  $n_{11}$  vs.  $\eta_2$     b)  $n_{12}$  vs.  $\eta_2$





(7a)



(7b)

*FIGURE 7.* The second normal stress  $n_{2i}$  in the two layers as functions of the network viscosity  $\eta$  of the upper layer for values of the network mobility parameter  $\alpha$  between 0.1 and 0.5. Case A where  $We_1 = We_2 = 1$ ,  $d_1 = d_2 = 0.5$ . The Newtonian viscosity are zero, the network viscosity of the lower layer is fixed at 1.

a)  $n_{21}$  vs.  $\eta_2$     b)  $n_{22}$  vs.  $\eta_2$ .

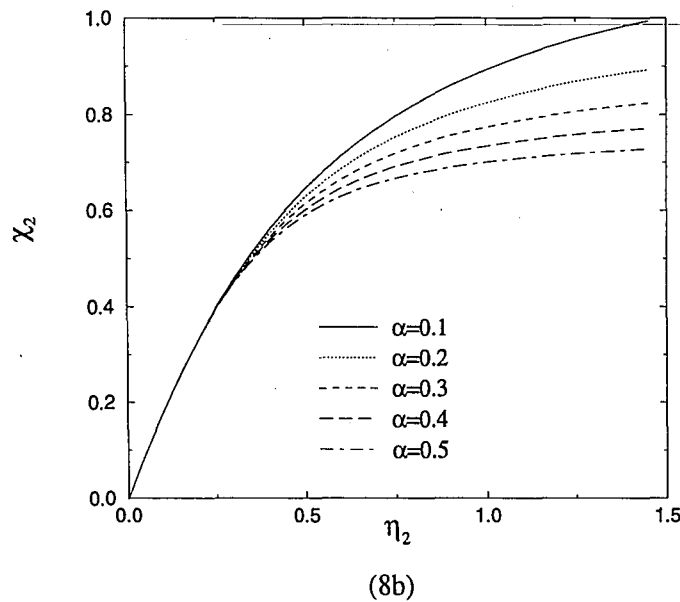
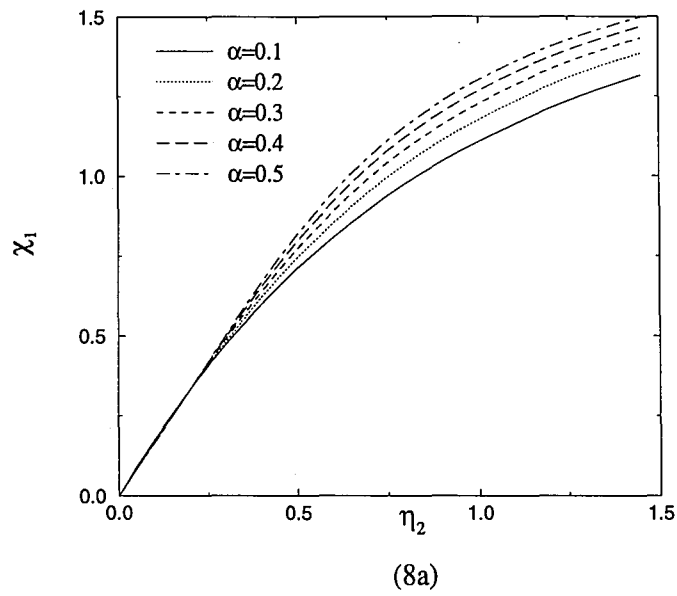


*FIGURE 8.* The velocity gradients  $\chi_i$  in the two layers as functions of the network viscosity  $\eta$  of the upper layer for values of the network mobility parameter  $\alpha$  between 0.1 and 0.5. Case B where  $We_1 = 1$   $We_2 = 0.2$ ,  $d_1 = d_2 = 0.5$ . The Newtonian viscosity are zero, the network viscosity of the lower layer is fixed at 1.

a)  $\chi_1$  vs.  $\eta_2$     b)  $\chi_2$  vs.  $\eta_2$

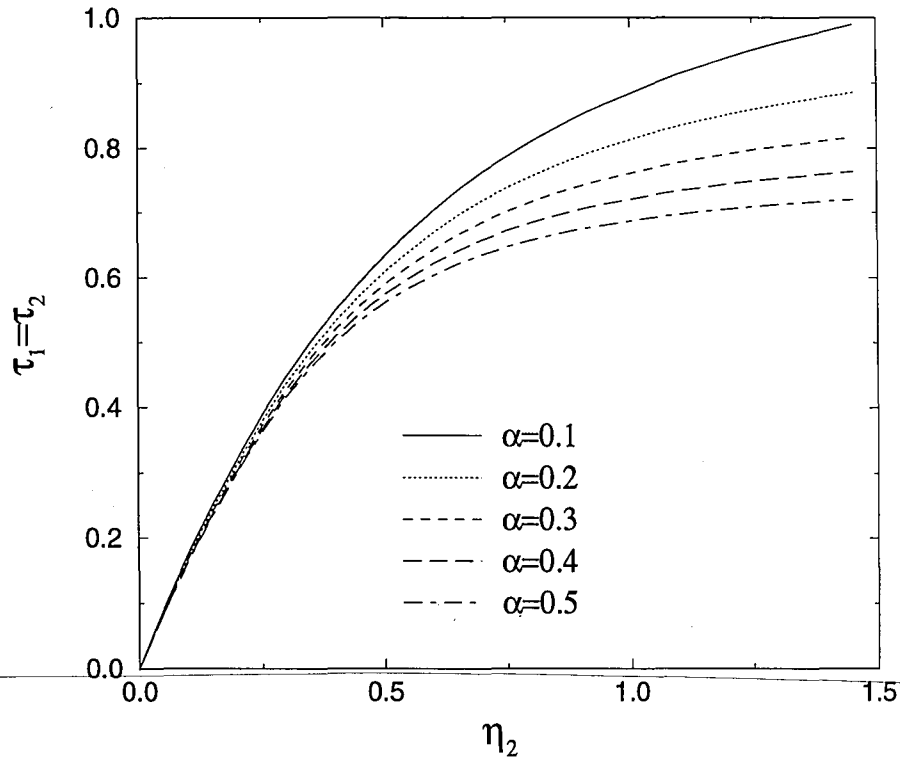


*FIGURE 9.* The shear stress  $\tau_i$  in the two layers as functions of the network viscosity  $\eta$  of the upper layer for values of the network mobility parameter  $\alpha$  between 0.1 and 0.5. Case B where  $We_1 = 1$   $We_2 = 0.2$ ,  $d_1 = d_2 = 0.5$ . The Newtonian viscosity are zero, the network viscosity of the lower layer is fixed at 1.

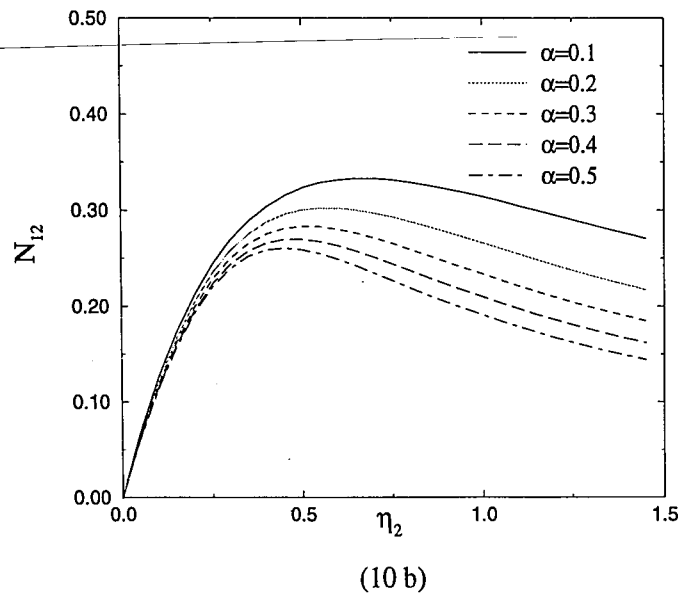
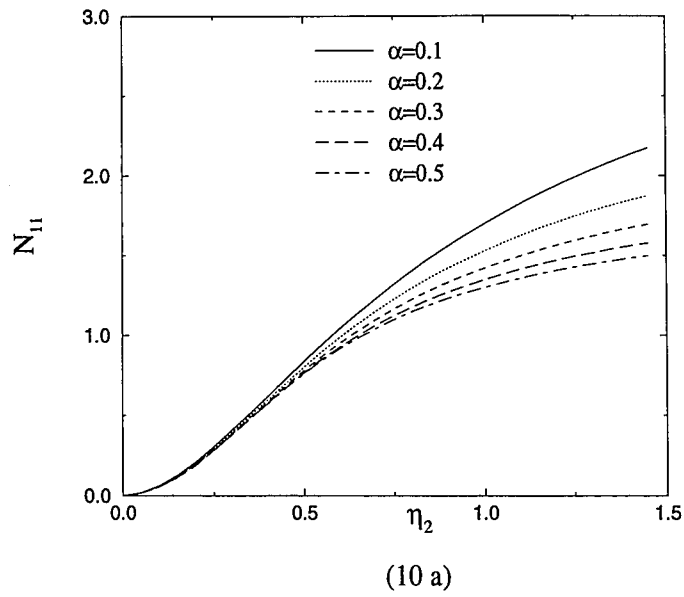
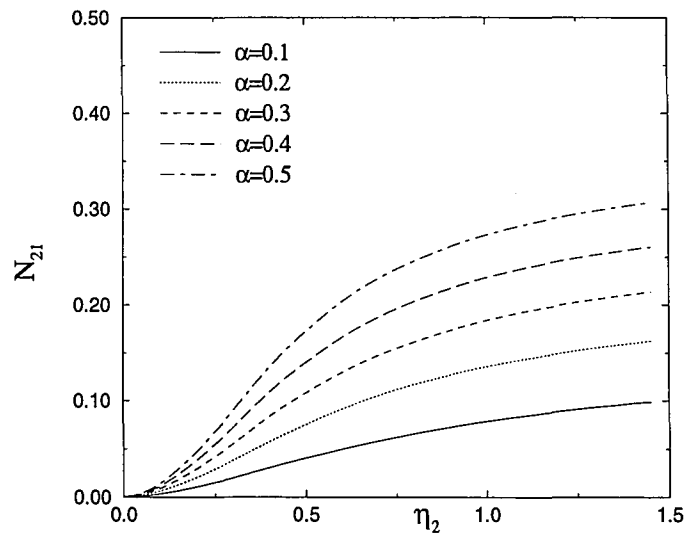
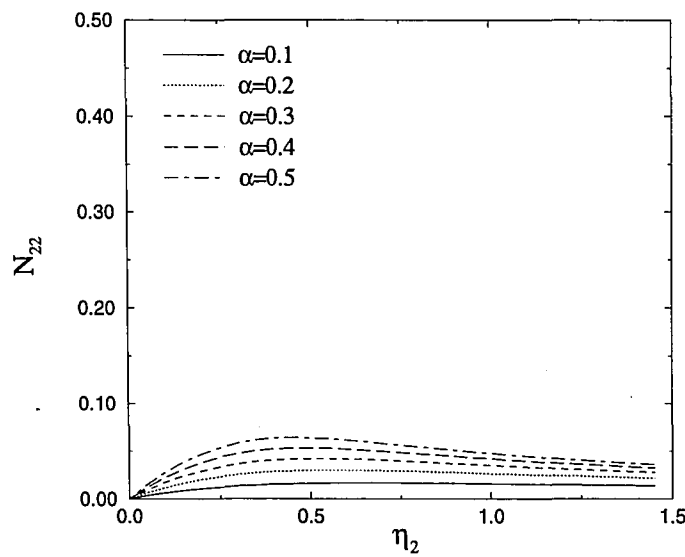


*FIGURE 10.* The first normal stress  $n_{1i}$  in the two layers as functions of the network viscosity  $\eta$  of the upper layer for values of the network mobility parameter  $\alpha$  between 0.1 and 0.5. Case B where  $We_1 = 1$   $We_2 = 0.2$ ,  $d_1 = d_2 = 0.5$ . The Newtonian viscosity are zero, the network viscosity of the lower layer is fixed at 1.

a)  $n_{11}$  vs.  $\eta_2$     b)  $n_{12}$  vs.  $\eta_2$



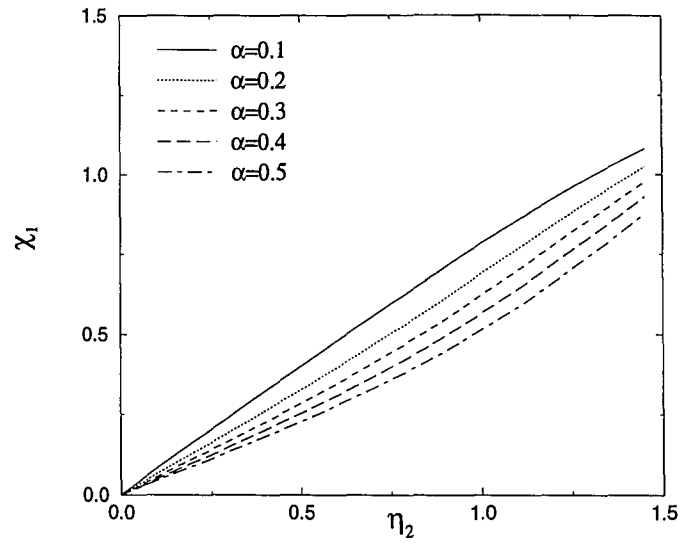
(11 a)



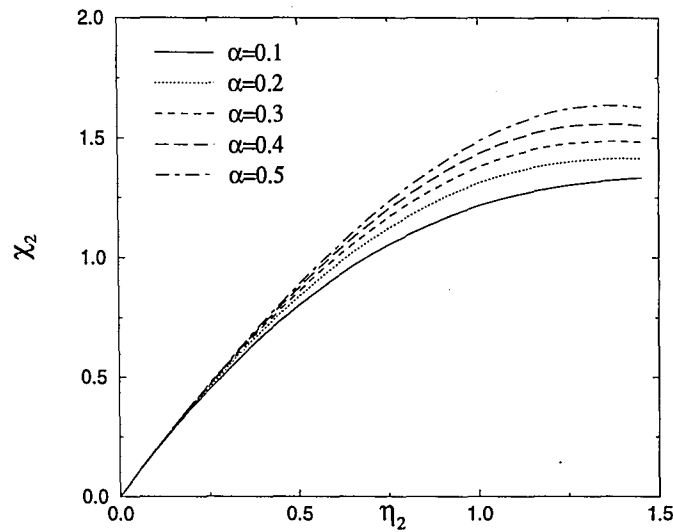
(11 b)

*FIGURE 11.* The second normal stress  $n_{2i}$  in the two layers as functions of the network viscosity  $\eta$  of the upper layer for values of the network mobility parameter  $\alpha$  between 0.1 and 0.5. Case B where  $We_1 = 1$   $We_2 = 0.2$ ,  $d_1 = d_2 = 0.5$ . The Newtonian viscosity are zero, the network viscosity of the lower layer is fixed at 1.

a)  $n_{21}$  vs.  $\eta_2$     b)  $n_{22}$  vs.  $\eta_2$



(12 a)



(12 b)

*FIGURE 12.* The velocity gradients  $\chi_i$  in the two layers as functions of the network viscosity  $\eta$  of the upper layer for values of the network mobility parameter  $\alpha$  between 0.1 and 0.5. Case C where  $We_1 = 1$   $We_2 = 2$ ,  $d_1 = d_2 = 0.5$ . The Newtonian viscosities are zero, the network viscosity of the lower layer is fixed at 1.

a)  $\chi_1$  vs.  $\eta_2$     b)  $\chi_2$  vs.  $\eta_2$

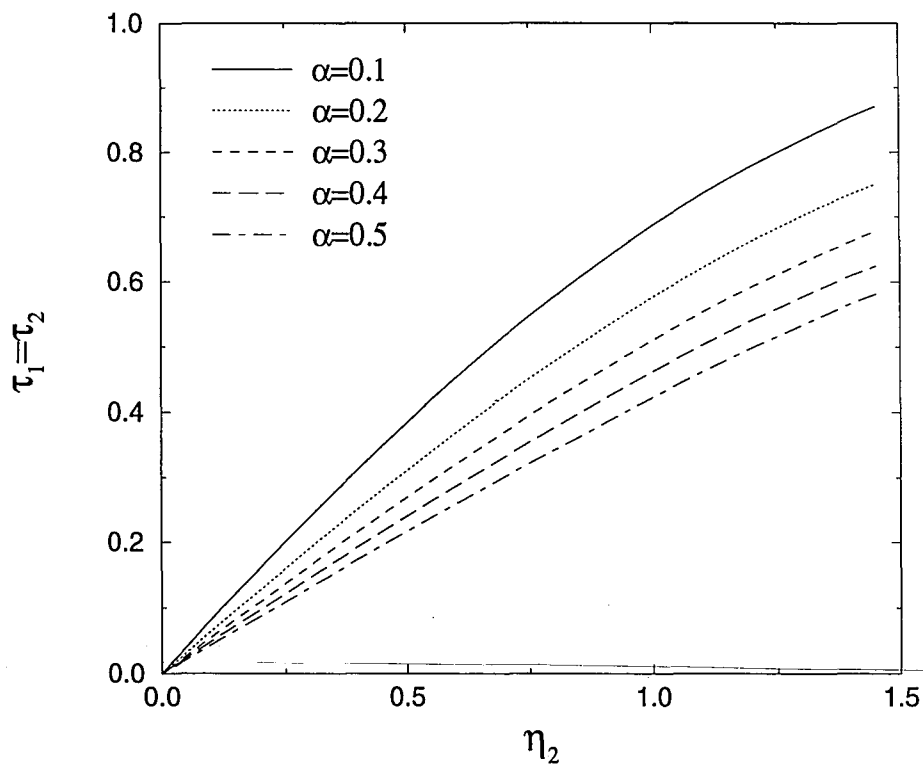
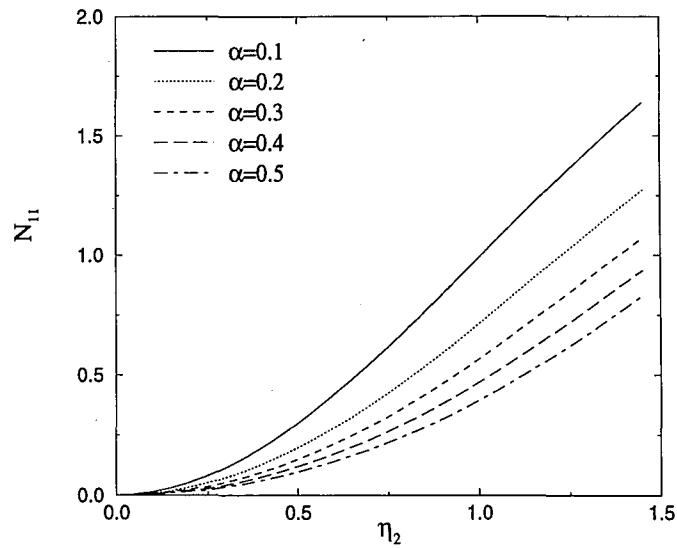
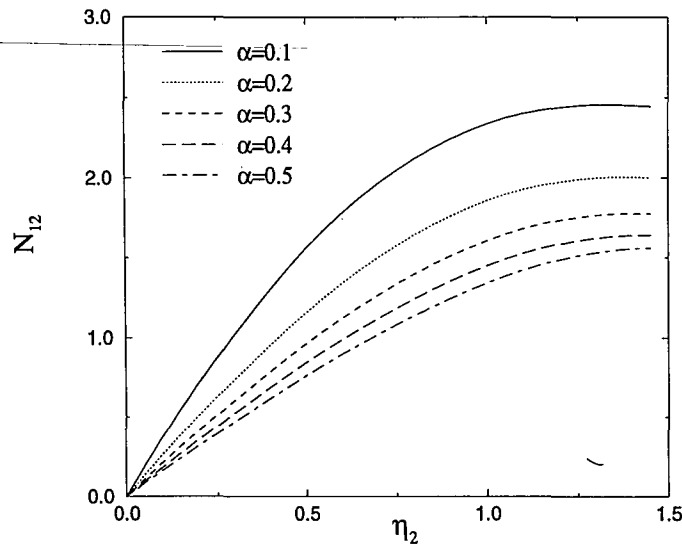


*FIGURE 13.* The shear stress  $\tau_i$  in the two layers as functions of the network viscosity  $\eta$  of the upper layer for values of the network mobility parameter  $\alpha$  between 0.1 and 0.5. Case C where  $We_1 = 1$ ,  $we_2 = 2$ ,  $d_1 = d_2 = 0.5$ . The Newtonian viscosity are zero, the network viscosity of the lower layer is fixed at 1.



(14 a)

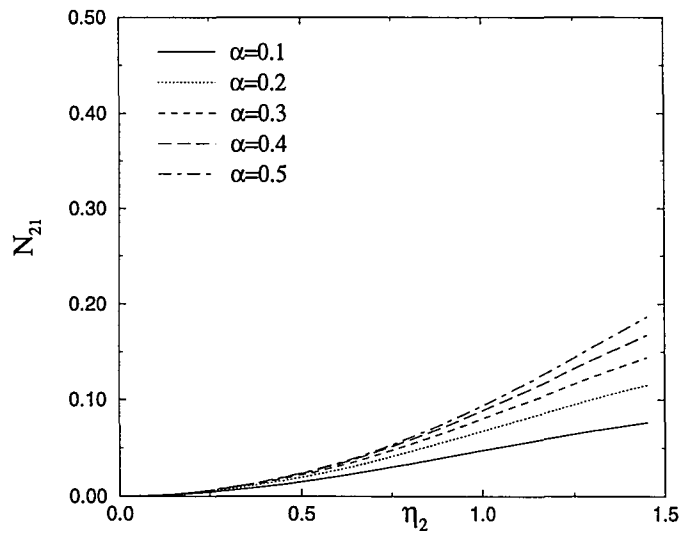


(14 b)

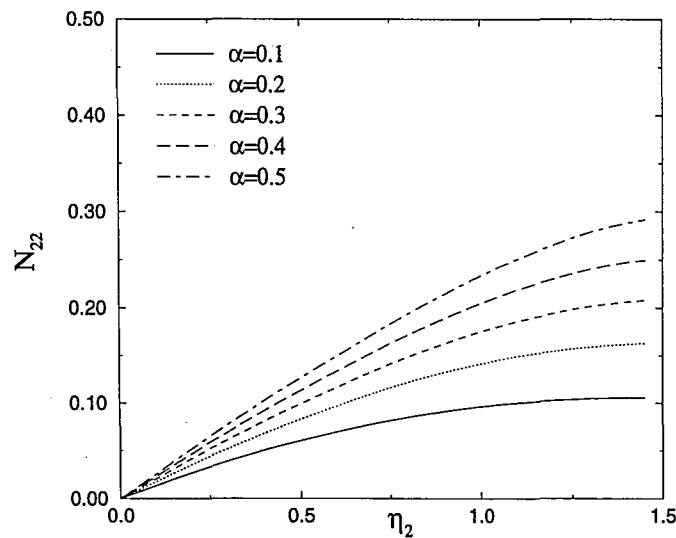
*FIGURE 14.* The first normal stress  $n_{1i}$  in the two layers as functions of the network viscosity  $\eta$  of the upper layer for values of the network mobility parameter  $\alpha$  between 0.1 and 0.5. Case C where  $We_1 = 1$   $We_2 = 2$ ,  $d_1 = d_2 = 0.5$ . The Newtonian viscosity are zero, the network viscosity of the lower layer is fixed at 1.

a)  $n_{11}$  vs.  $\eta_2$     b)  $n_{12}$  vs.  $\eta_2$





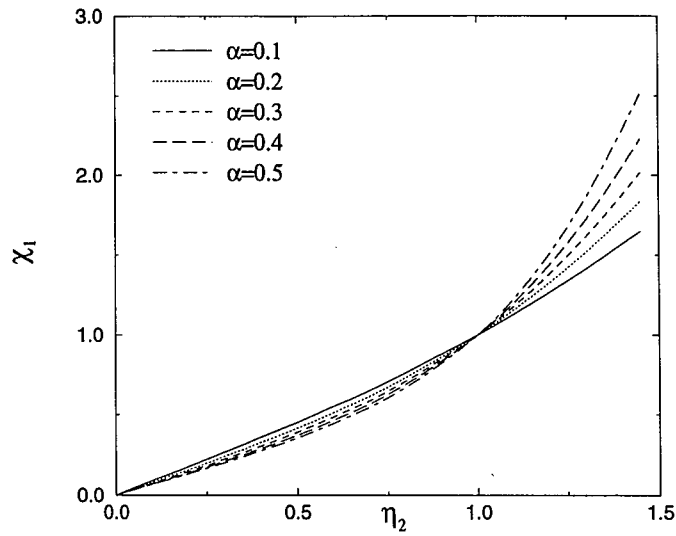
(15 a)



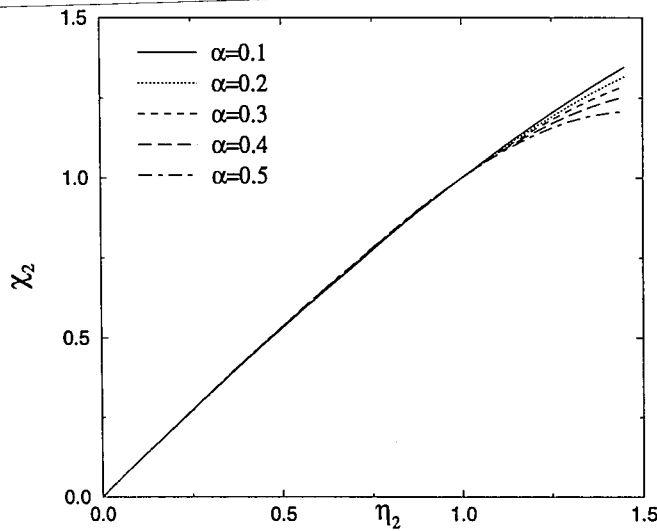
(15 b)

*FIGURE 15.* The second normal stress  $n_{2i}$  in the two layers as functions of the network viscosity  $\eta$  of the upper layer for values of the network mobility parameter  $\alpha$  between 0.1 and 0.5. Case C where  $We_1 = 1$   $We_2 = 2$ ,  $d_1 = d_2 = 0.5$ . The Newtonian viscosity are zero, the network viscosity of the lower layer is fixed at 1.

a)  $n_{21}$  vs.  $\eta_2$     b)  $n_{22}$  vs.  $\eta_2$



(16 a)



(16b)

**FIGURE 16.** The velocity gradients  $\chi_i$  in the two layers as functions of the network viscosity  $\eta$  of the upper layer for values of the network mobility parameter  $\alpha$  between 0.1 and 0.5. Case D where  $We_1 = We_2 = 1$ ,  $d_1 = 0.1$   $d_2 = 0.9$ . The Newtonian viscosity are zero, the network viscosity of the lower layer is fixed at 1.

a)  $\chi_1$  vs.  $\eta_2$     b)  $\chi_2$  vs.  $\eta_2$ .

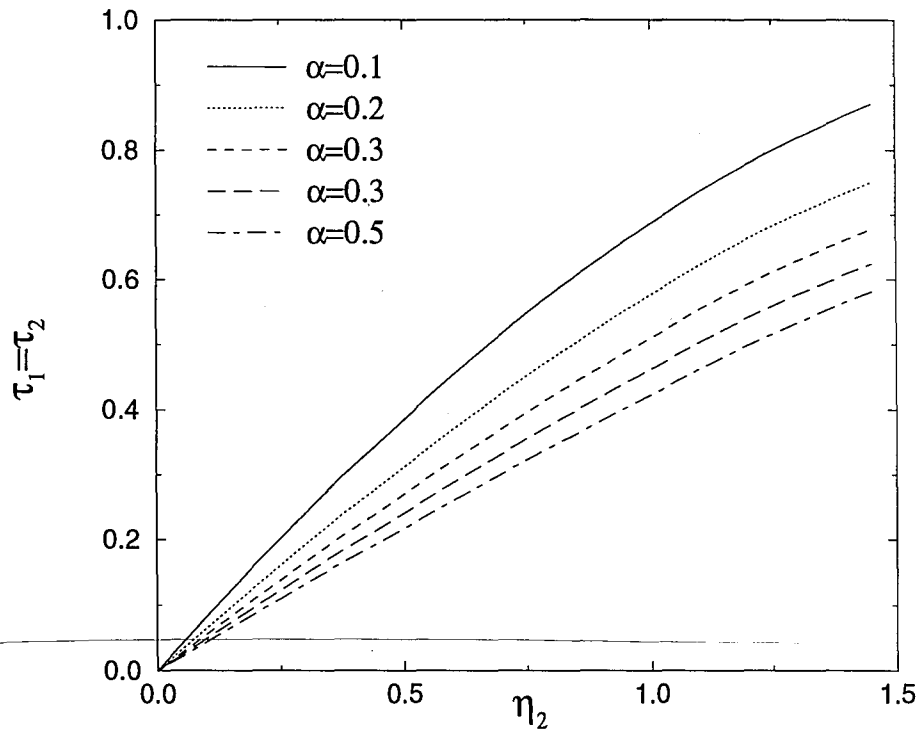
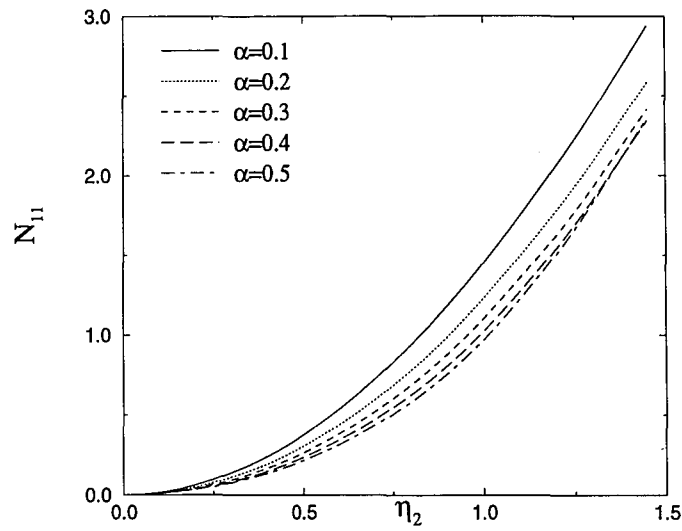
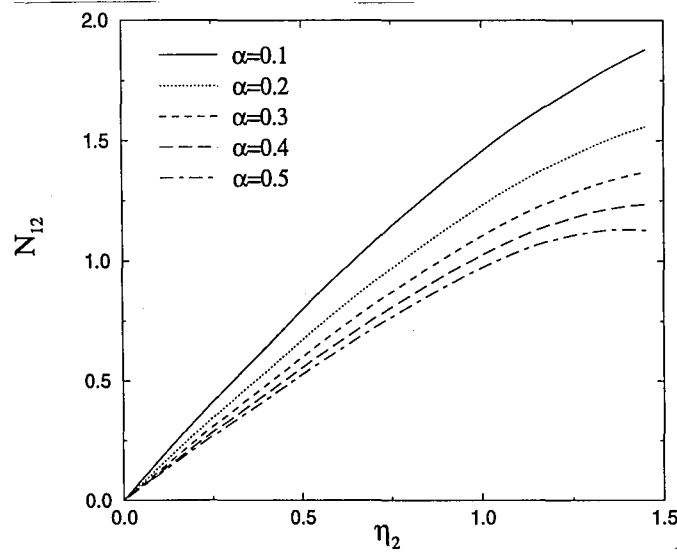


*FIGURE 17.* The shear stress  $\tau_i$  in the two layers as functions of the network viscosity  $\eta$  of the upper layer for values of the network mobility parameter  $\alpha$  between 0.1 and 0.5. Case D where  $We_1 = We_2 = 1$ ,  $d_1 = 0.1$   $d_2 = 0.9$ . The Newtonian viscosity are zero, the network viscosity of the lower layer is fixed at 1.



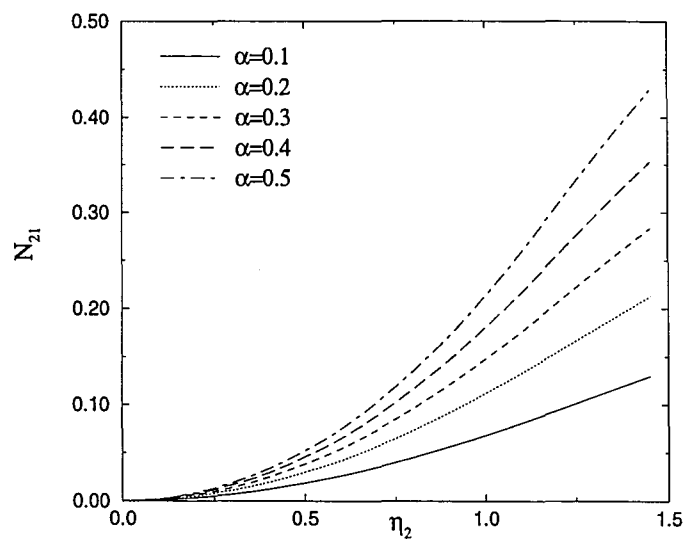
(18 a)



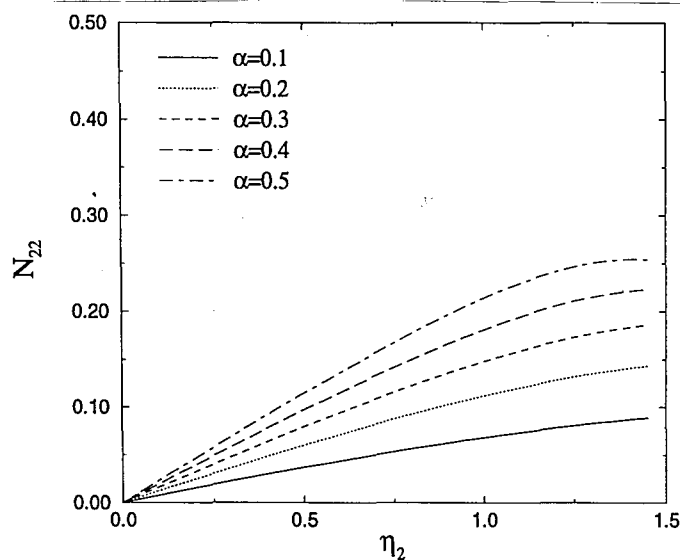
(18 b)

*FIGURE 18.* The first normal stress  $n_{1i}$  in the two layers as functions of the network viscosity  $\eta$  of the upper layer for values of the network mobility parameter  $\alpha$  between 0.1 and 0.5. Case D where  $We_1 = We_2 = 1$ ,  $d_1 = 0.1$   $d_2 = 0.9$ . The Newtonian viscosity are zero, the network viscosity of the lower layer is fixed at 1.

a)  $n_{11}$  vs.  $\eta_2$     b)  $n_{12}$  vs.  $\eta_2$



(19 a)



(19 b)

**FIGURE 19.** The second normal stress  $n_{2i}$  in the two layers as functions of the network viscosity  $\eta$  of the upper layer for values of the network mobility parameter  $\alpha$  between 0.1 and 0.5. Case D where  $We_1 = We_2 = 1$ ,  $d_1 = 0.1$   $d_2 = 0.9$ . The Newtonian viscosity are zero, the network viscosity of the lower layer is fixed at 1.

a)  $n_{21}$  vs.  $\eta_2$     b)  $n_{22}$  vs.  $\eta_2$

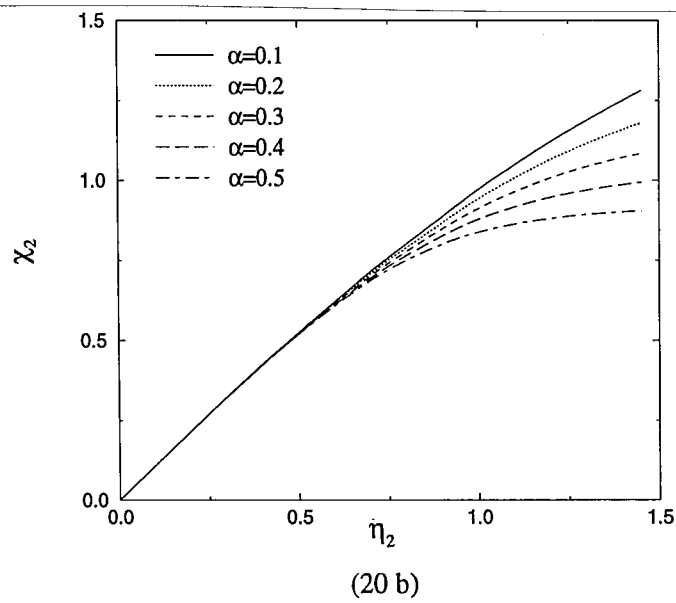
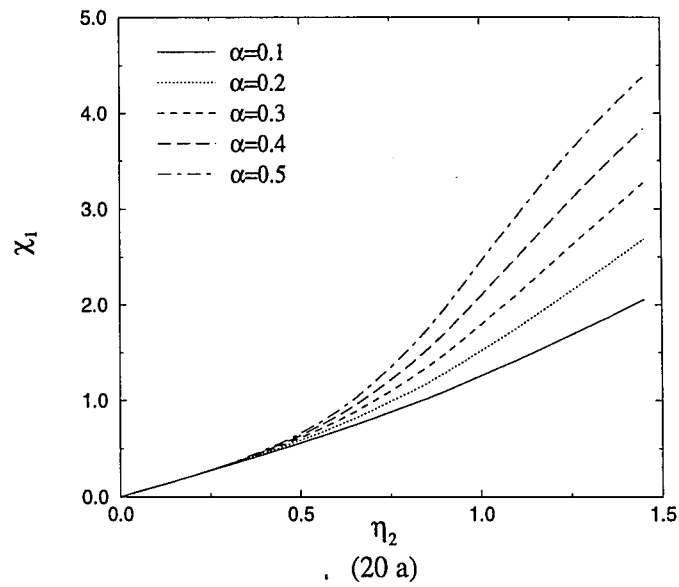


*FIGURE 20.* The velocity gradients  $\chi_i$  in the two layers as functions of the network viscosity  $\eta$  of the upper layer for values of the network mobility parameter  $\alpha$  between 0.1 and 0.5. Case E where  $We_1 = 1$   $We_2 = 0.2$ ,  $d_1 = 0.1$   $d_2 = 0.9$ . The Newtonian viscosity are zero, the network viscosity of the lower layer is fixed at 1.

a)  $\chi_1$  vs.  $\eta_2$     b)  $\chi_2$  vs.  $\eta_2$

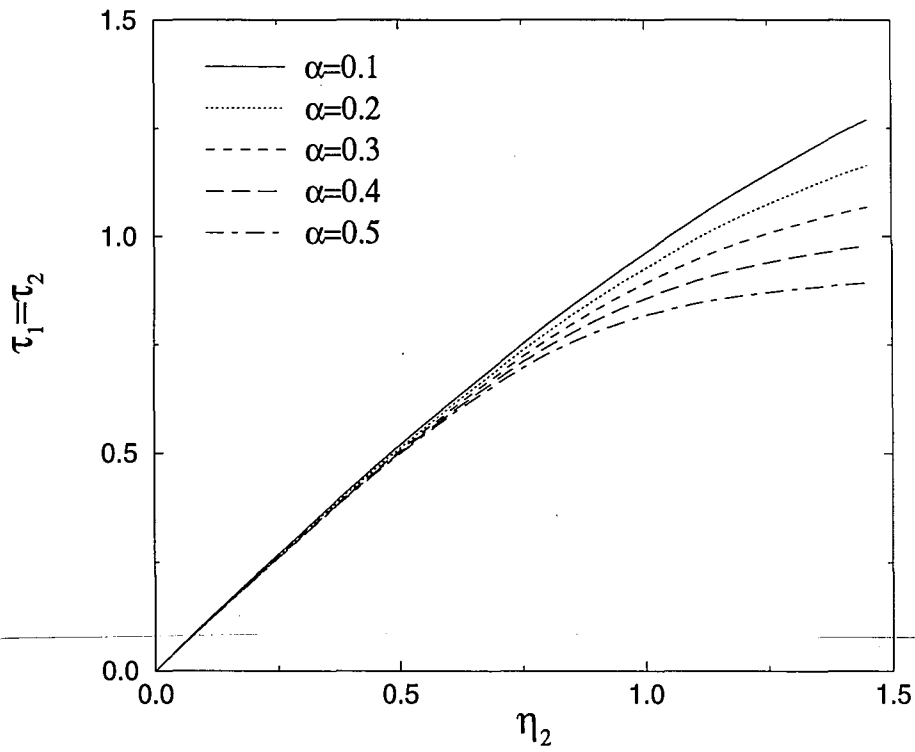
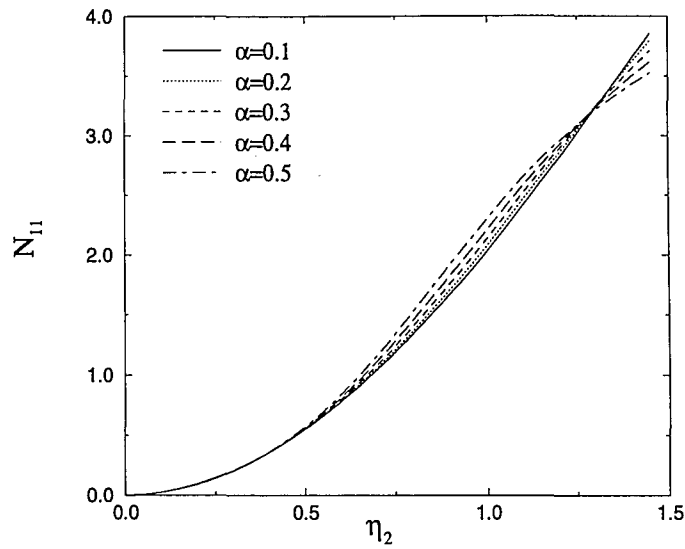
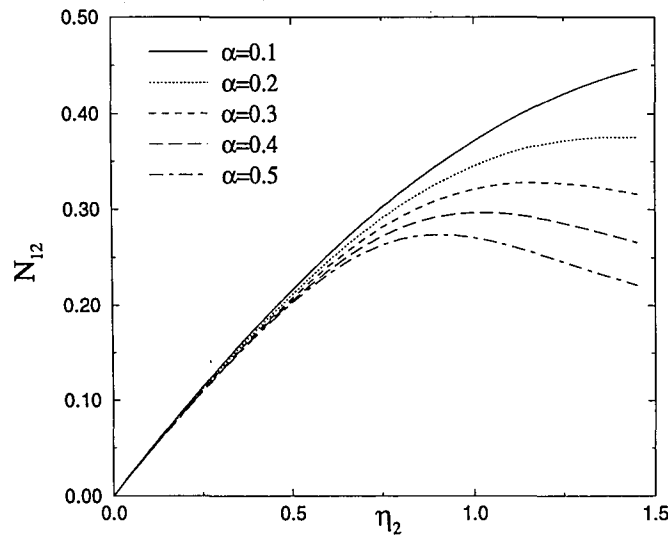


*FIGURE 21.* The shear stress  $\tau_i$  in the two layers as functions of the network viscosity  $\eta$  of the upper layer for values of the network mobility parameter  $\alpha$  between 0.1 and 0.5. Case E where  $We_1 = 1$   $We_2 = 0.2$ ,  $d_1 = 0.1$   $d_2 = 0.9$ . The Newtonian viscosity are zero, the network viscosity of the lower layer is fixed at 1.



(22 a)

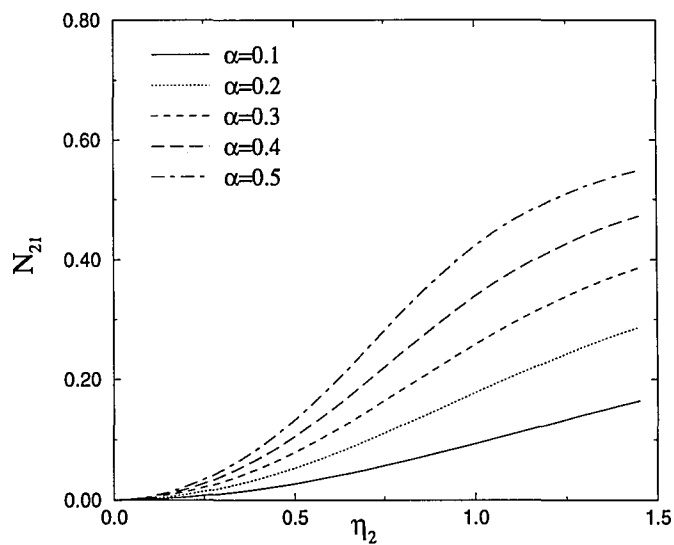


(22b)

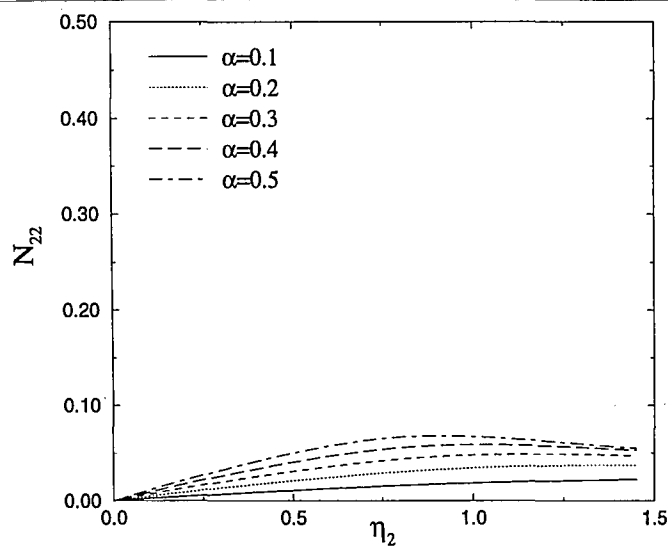
*FIGURE 22.* The first normal stress  $n_{1i}$  in the two layers as functions of the network viscosity  $\eta$  of the upper layer for values of the network mobility parameter  $\alpha$  between 0.1 and 0.5. Case E where  $We_1 = 1$   $We_2 = 0.2$ ,  $d_1 = 0.1$   $d_2 = 0.9$ . The Newtonian viscosity are zero, the network viscosity of the lower layer is fixed at 1.

a)  $n_{11}$  vs.  $\eta_2$     b)  $n_{12}$  vs.  $\eta_2$





(23 a)



(23 b)

*FIGURE 23.* The second normal stress  $n_{2i}$  in the two layers as functions of the network viscosity  $\eta$  of the upper layer for values of the network mobility parameter  $\alpha$  between 0.1 and 0.5. Case E where  $We_1 = 1$   $We_2 = 0.2$ ,  $d_1 = 0.1$   $d_2 = 0.9$ . The Newtonian viscosity are zero, the network viscosity of the lower layer is fixed at 1.

a)  $n_{21}$  vs.  $\eta_2$     b)  $n_{22}$  vs.  $\eta_2$

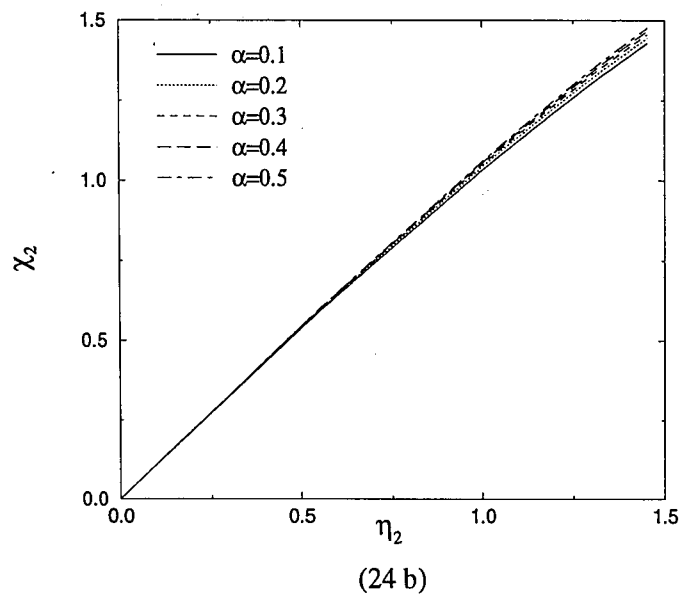
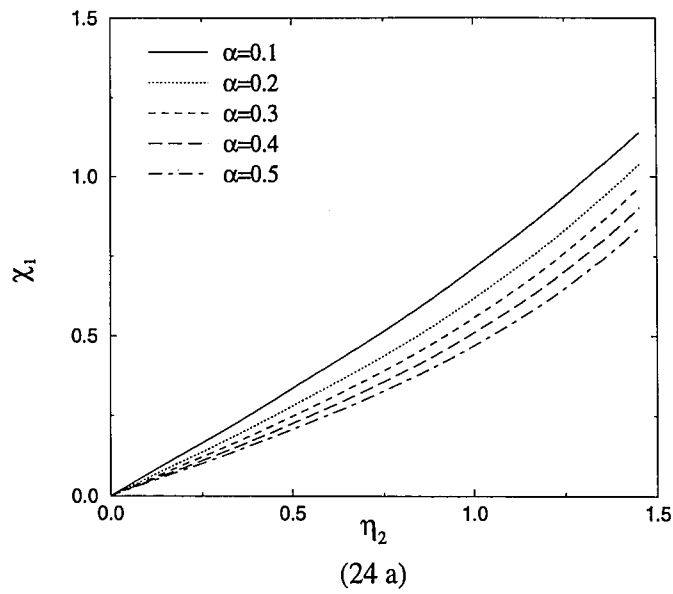


*FIGURE 24.* The velocity gradients  $\chi_i$  in the two layers as functions of the network viscosity  $\eta$  of the upper layer for values of the network mobility parameter  $\alpha$  between 0.1 and 0.5. Case F where  $We_1 = 1$   $We_2 = 2$ ,  $d_1 = 0.1$   $d_2 = 0.9$ . The Newtonian viscosity are zero, the network viscosity of the lower layer is fixed at 1.

a)  $\chi_1$  vs.  $\eta_2$     b)  $\chi_2$  vs.  $\eta_2$

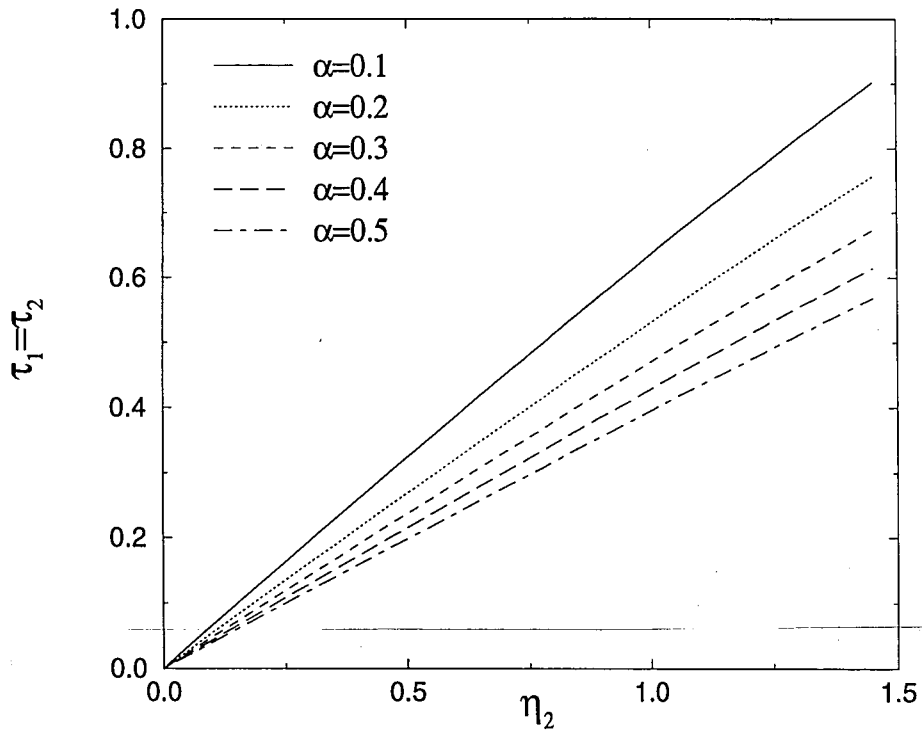
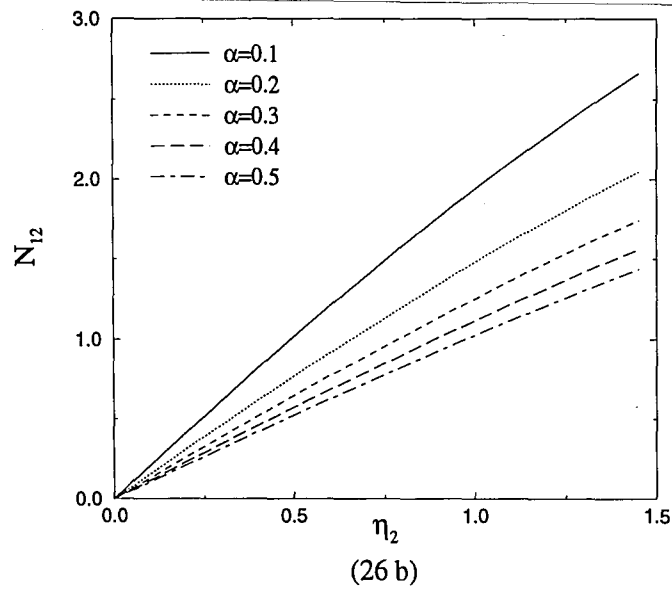
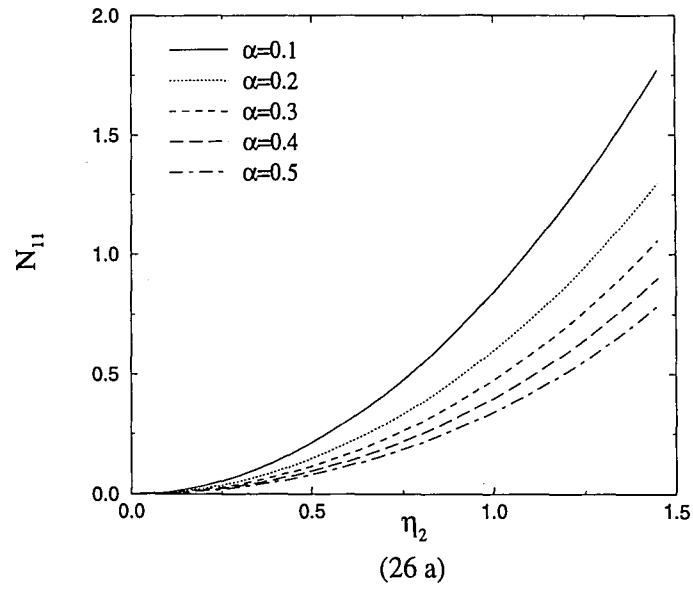
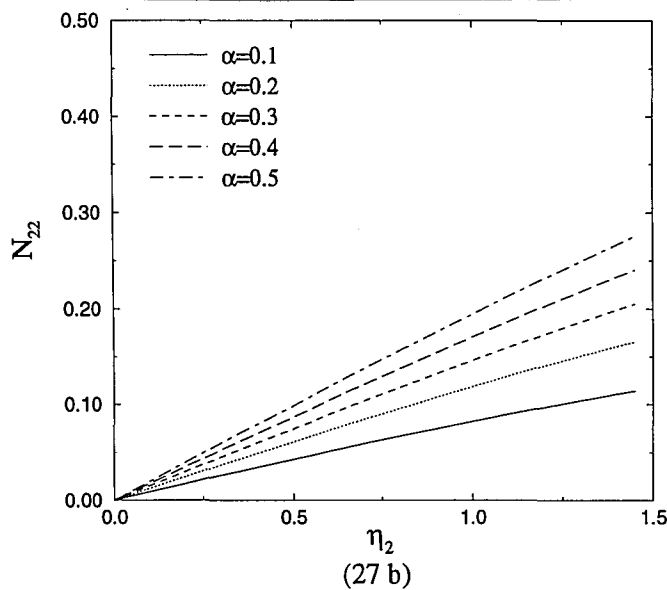
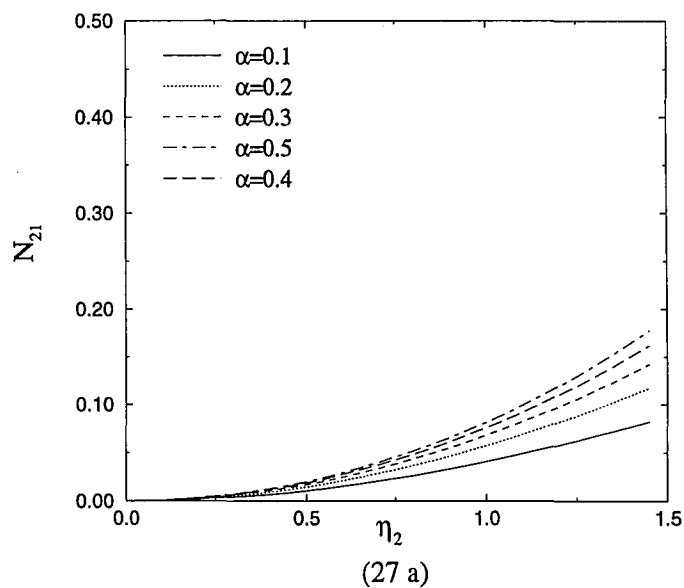


FIGURE 25. The shear stress  $\tau_i$  in the two layers as functions of the network viscosity  $\eta$  of the upper layer for values of the network mobility parameter  $\alpha$  between 0.1 and 0.5. Case F where  $We_1 = 1$   $We_2 = 2$ ,  $d_1 = 0.1$   $d_2 = 0.9$ . The Newtonian viscosity are zero, the network viscosity of the lower layer is fixed at 1.



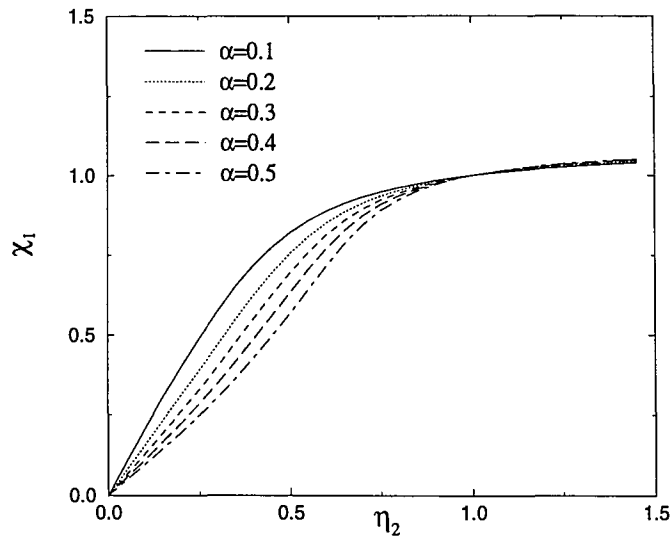
**FIGURE 26.** The first normal stress  $n_{1i}$  in the two layers as functions of the network viscosity  $\eta$  of the upper layer for values of the network mobility parameter  $\alpha$  between 0.1 and 0.5. Case F where  $We_1 = 1$   $We_2 = 2$ ,  $d_1 = 1$   $d_2 = 0.9$ . The Newtonian viscosity are zero, the network viscosity of the lower layer is fixed at 1.

a)  $n_{11}$  vs.  $\eta_2$     b)  $n_{12}$  vs.  $\eta_2$

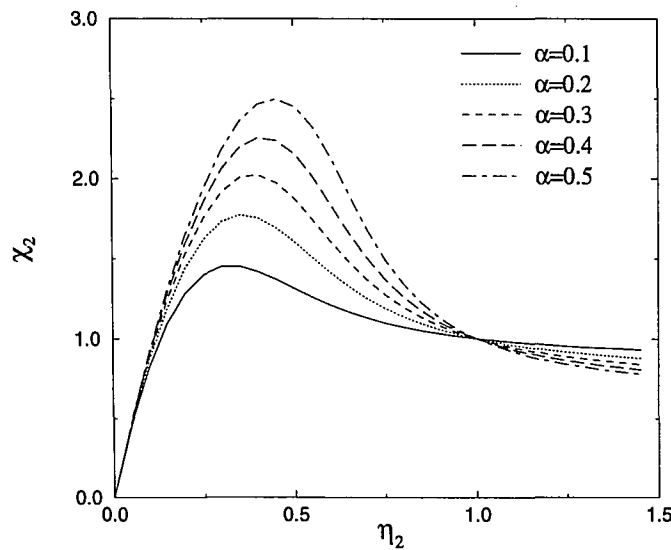


*FIGURE 27.* The second normal stress  $n_{2i}$  in the two layers as functions of the network viscosity  $\eta$  of the upper layer for values of the network mobility parameter  $\alpha$  between 0.1 and 0.5. Case F where  $We_1 = 1$   $We_2 = 2$ ,  $d_1 = 0.1$   $d_2 = 0.9$ . The Newtonian viscosity are zero, the network viscosity of the lower layer is fixed at 1.

a)  $n_{21}$  vs.  $\eta_2$     b)  $n_{22}$  vs.  $\eta_2$



(28 a)



(28 b)

**FIGURE 28.** The velocity gradients  $\chi_i$  in the two layers as functions of the network viscosity  $\eta$  of the upper layer for values of the network mobility parameter  $\alpha$  between 0.1 and 0.5. Case G where  $We_1 = We_2 = 1$ ,  $d_1 = 0.9$   $d_2 = 0.1$ . The Newtonian viscosity are zero, the network viscosity of the lower layer is fixed at 1.

a)  $\chi_1$  vs.  $\eta_2$     b)  $\chi_2$  vs.  $\eta_2$

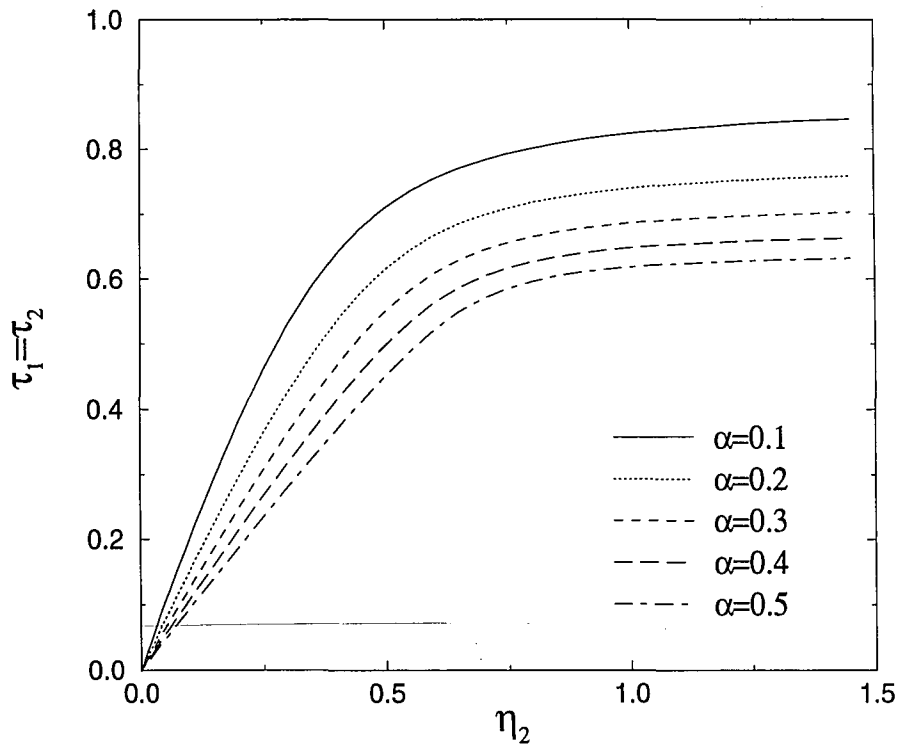
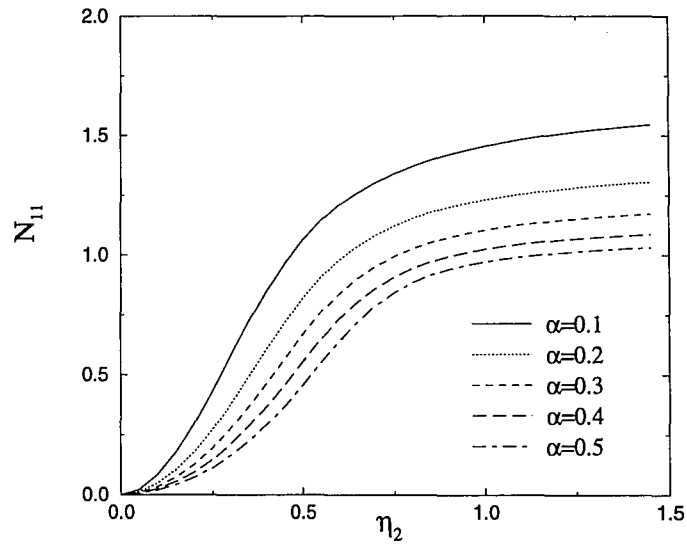
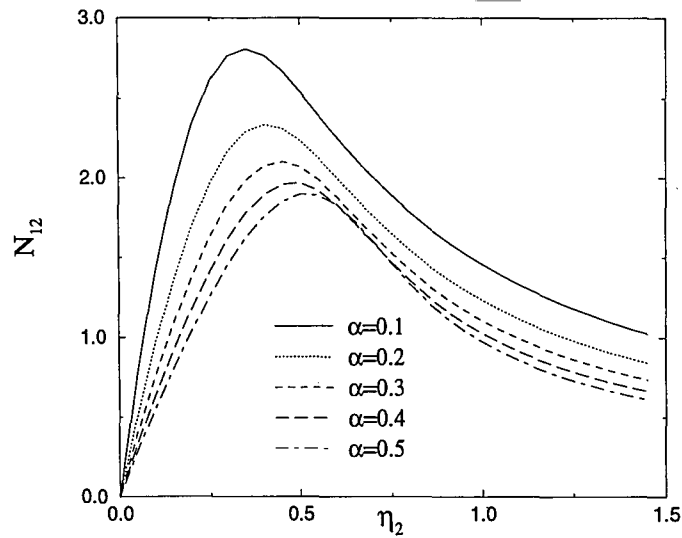


*FIGURE 29.* The shear stress  $\tau_i$  in the two layers as functions of the network viscosity  $\eta$  of the upper layer for values of the network mobility parameter  $\alpha$  between 0.1 and 0.5. Case G where  $We_1 = We_2 = 1$ ,  $d_1 = 0.9$   $d_2 = 0.1$ . The Newtonian viscosity are zero, the network viscosity of the lower layer is fixed at 1.



(30 a)



(30 b)

*FIGURE 30.* The first normal stress  $n_{1i}$  in the two layers as functions of the network viscosity  $\eta$  of the upper layer for values of the network mobility parameter  $\alpha$  between 0.1 and 0.5. Case G where  $We_1 = We_2 = 1$ ,  $d_1 = 0.9$   $d_2 = 0.1$ . The Newtonian viscosity are zero, the network viscosity of the lower layer is fixed at 1.

a)  $n_{11}$  vs.  $\eta_2$     b)  $n_{12}$  vs.  $\eta_2$



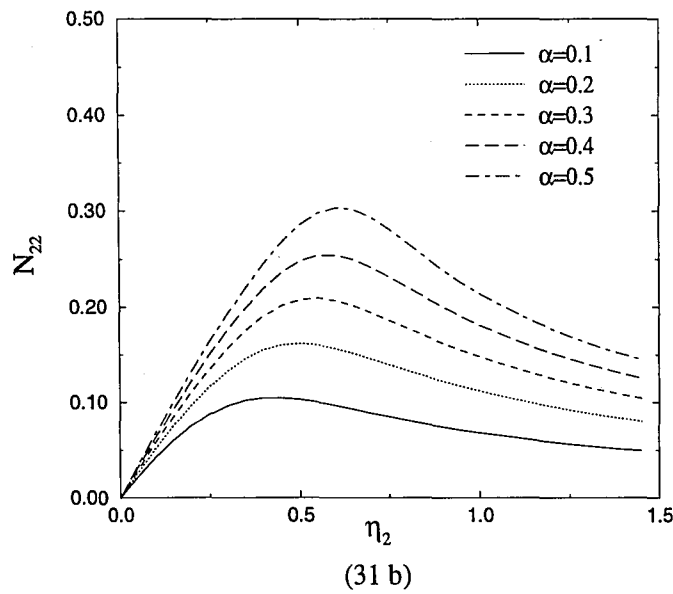
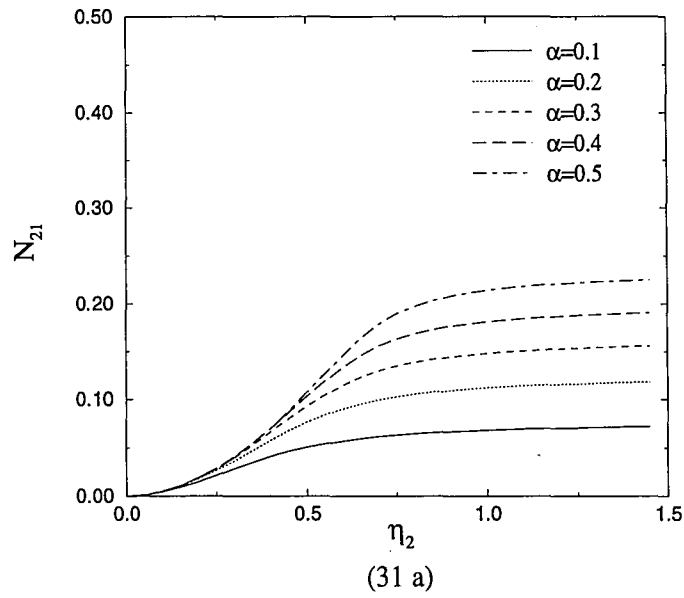
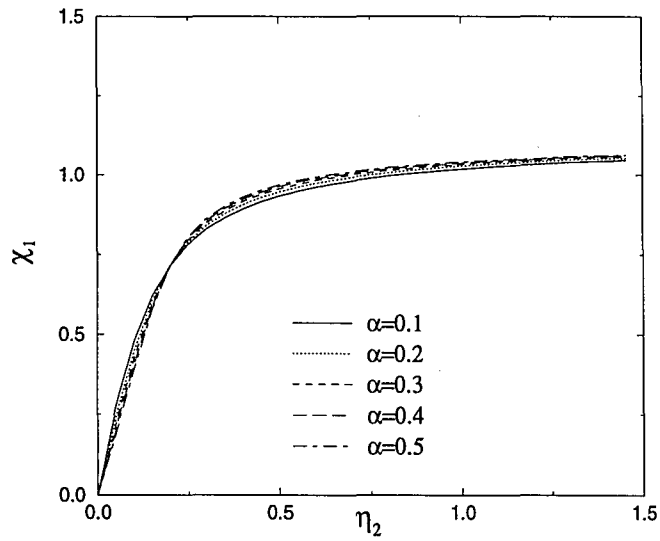
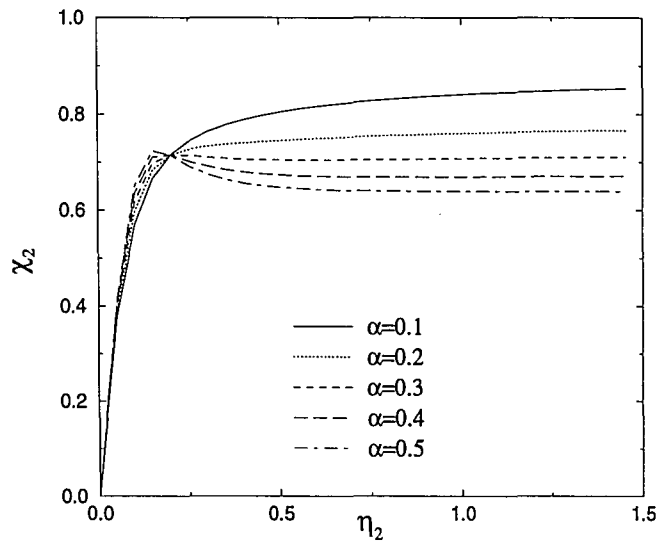


*FIGURE 31.* The second normal stress  $n_{2i}$  in the two layers as functions of the network viscosity  $\eta$  of the upper layer for values of the network mobility parameter  $\alpha$  between 0.1 and 0.5. Case G where  $We_1 = We_2 = 1$ ,  $d_1 = 0.9$   $d_2 = 0.1$ . The Newtonian viscosity are zero, the network viscosity of the lower layer is fixed at 1.

a)  $n_{21}$  vs.  $\eta_2$     b)  $n_{22}$  vs.  $\eta_2$



(32 a)



(32 b)

**FIGURE 32.** The velocity gradients  $\chi_i$  in the two layers as functions of the network viscosity  $\eta$  of the upper layer for values of the network mobility parameter  $\alpha$  between 0.1 and 0.5. Case H where  $We_1 = 1$   $We_2 = 0.2$ ,  $d_1 = 0.9$   $d_2 = 0.1$ . The Newtonian viscosities are zero, the network viscosity of the lower layer is fixed at 1.

a)  $\chi_1$  vs.  $\eta_2$     b)  $\chi_2$  vs.  $\eta_2$

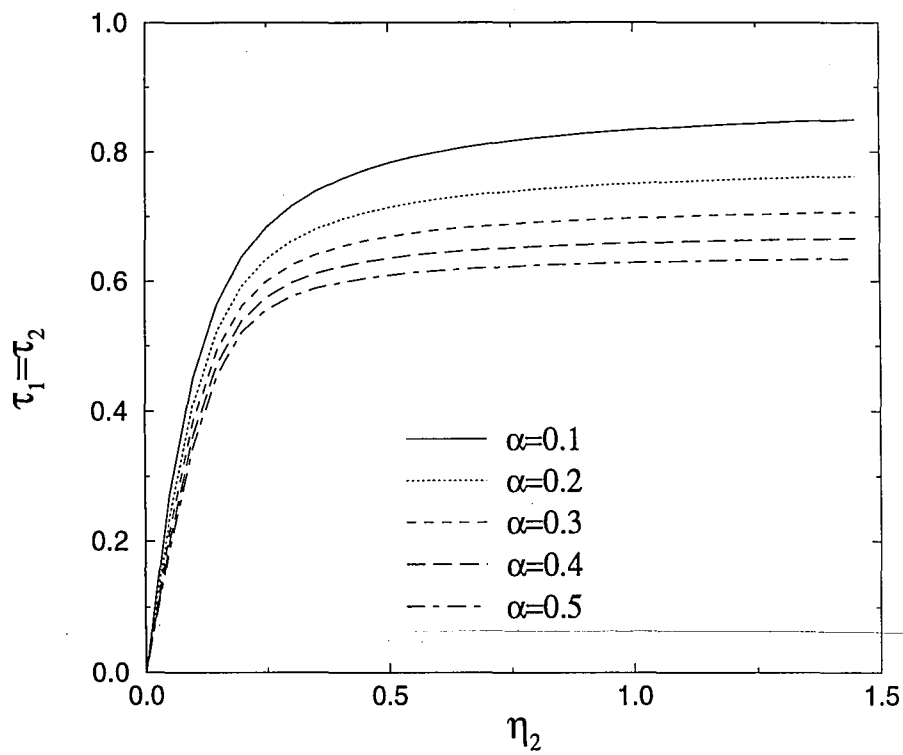


*FIGURE 33.* The shear stress  $\tau_i$  in the two layers as functions of the network viscosity  $\eta$  of the upper layer for values of the network mobility parameter  $\alpha$  between 0.1 and 0.5. Case H where  $We_1 = 1$   $We_2 = 0.2$ ,  $d_1 = 0.9$   $d_2 = 0.1$ . The Newtonian viscosity are zero, the network viscosity of the lower layer is fixed at 1.

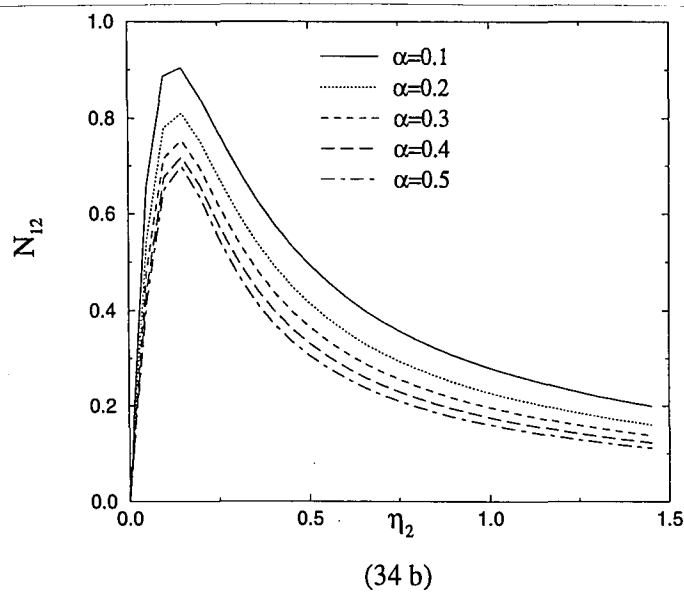
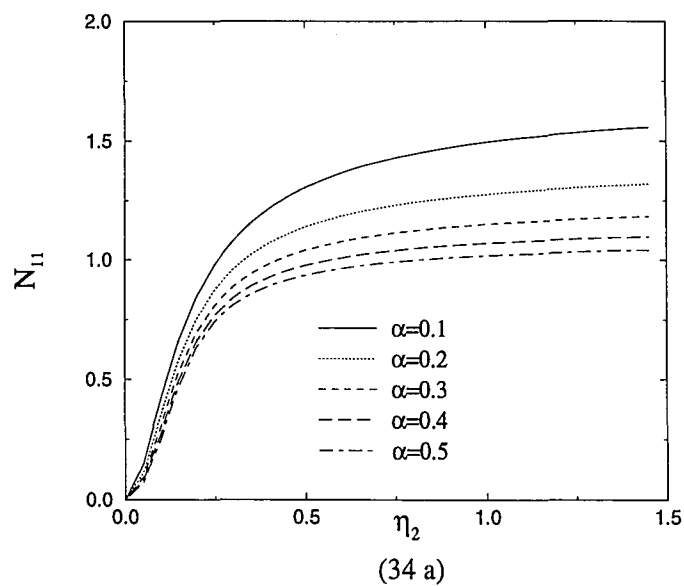


*FIGURE 34.* The first normal stress  $n_{1i}$  in the two layers as functions of the network viscosity  $\eta$  of the upper layer for values of the network mobility parameter  $\alpha$  between 0.1 and 0.5. Case H where  $We_1 = 1$   $We_2 = 0.2$ ,  $d_1 = 0.9$   $d_2 = 0.1$ . The Newtonian viscosity are zero, the network viscosity of the lower layer is fixed at 1.

a)  $n_{11}$  vs.  $\eta_2$     b)  $n_{12}$  vs.  $\eta_2$

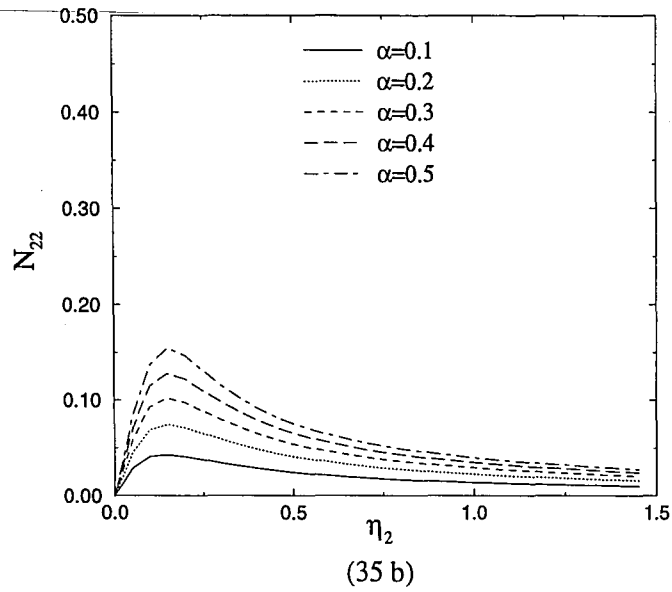
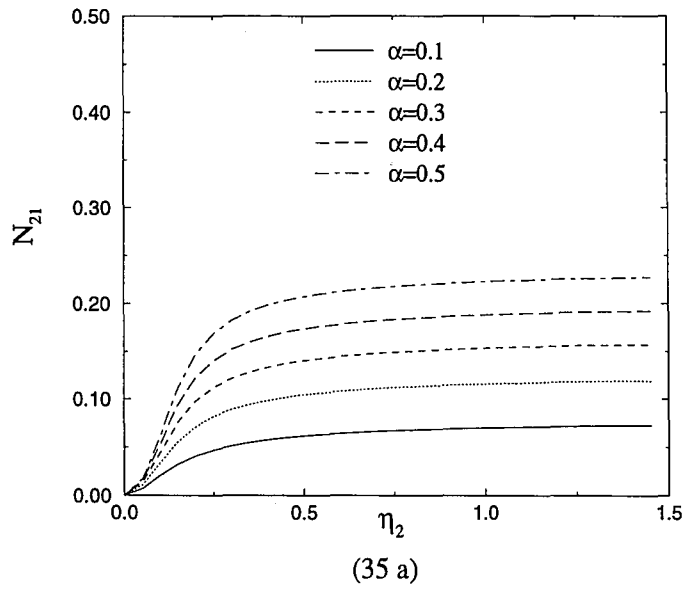
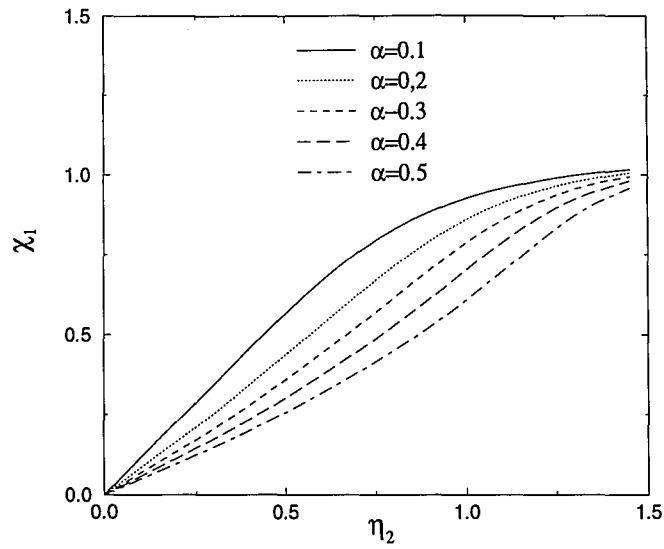
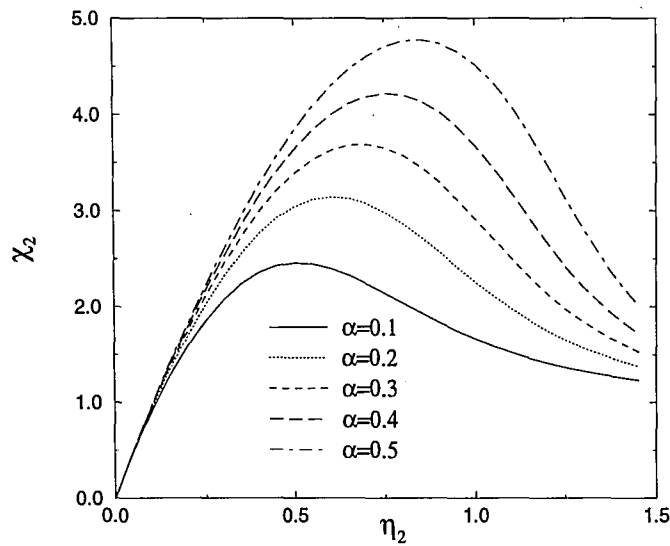


*FIGURE 35.* The second normal stress  $n_{2i}$  in the two layers as functions of the network viscosity  $\eta$  of the upper layer for values of the network mobility parameter  $\alpha$  between 0.1 and 0.5. Case H where  $We_1 = 1$   $We_2 = 0.2$ ,  $d_1 = 0.9$   $d_2 = 0.1$ . The Newtonian viscosity are zero, the network viscosity of the lower layer is fixed at 1.

a)  $n_{21}$  vs.  $\eta_2$     b)  $n_{22}$  vs.  $\eta_2$



(36 a)



(36 b)

**FIGURE 36.** The velocity gradients  $\chi_i$  in the two layers as functions of the network viscosity  $\eta$  of the upper layer for values of the network mobility parameter  $\alpha$  between 0.1 and 0.5. Case I where  $We_1 = 1$   $We_2 = 2$ ,  $d_1 = 0.9$   $d_2 = 0.1$ . The Newtonian viscosity are zero, the network viscosity of the lower layer is fixed at 1

.a)  $\chi_1$  vs.  $\eta_2$     b)  $\chi_2$  vs.  $\eta_2$

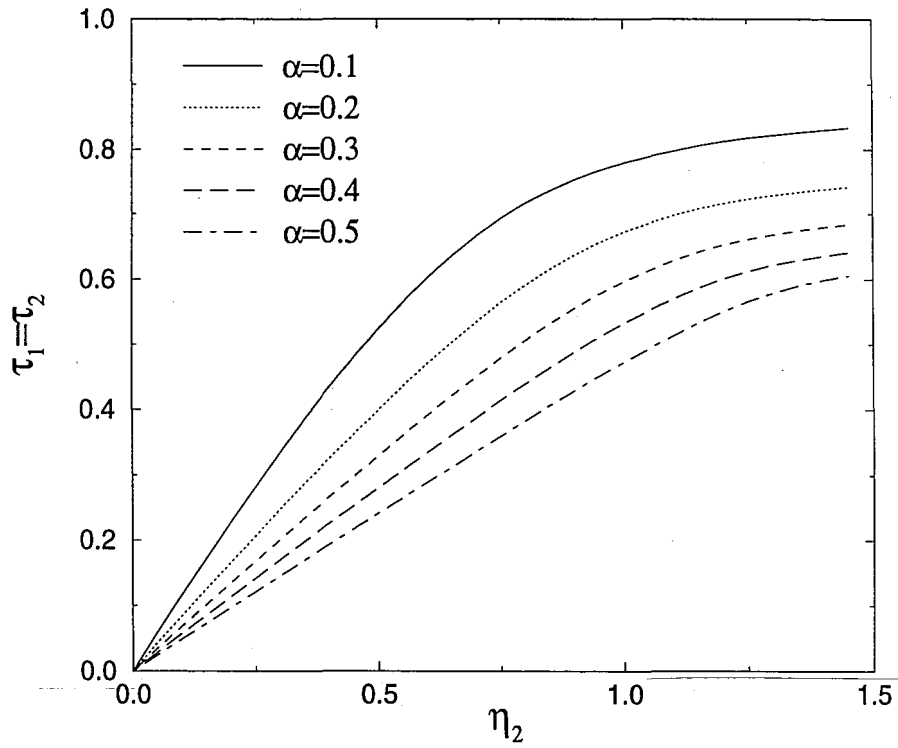


*FIGURE 37.* The shear stress  $\tau_i$  in the two layers as functions of the network viscosity  $\eta$  of the upper layer for values of the network mobility parameter  $\alpha$  between 0.1 and 0.5. Case I where  $We_1 = 1$   $We_2 = 2$ ,  $d_1 = 0.9$   $d_2 = 0.1$ . The Newtonian viscosity are zero, the network viscosity of the lower layer is fixed at 1.

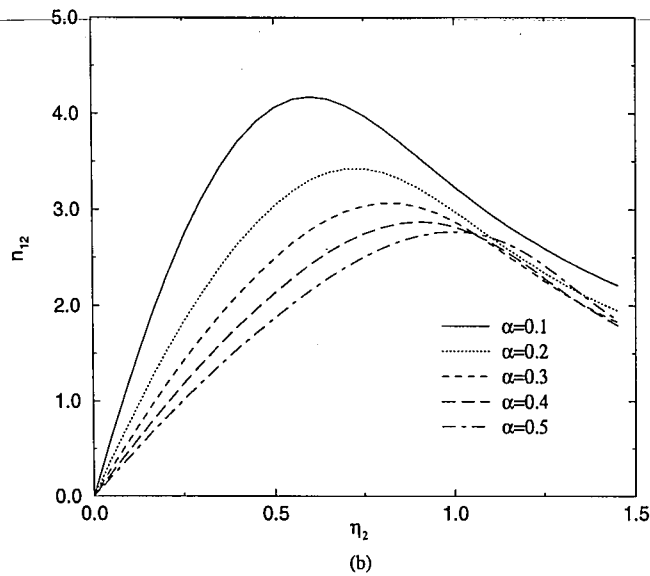
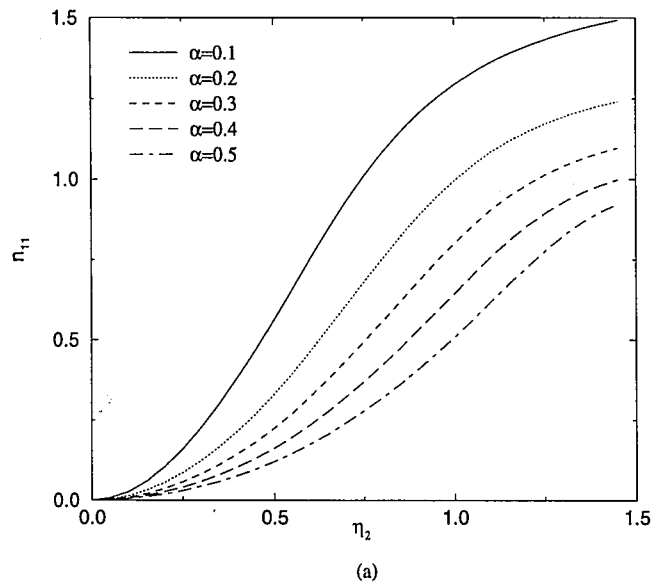


*FIGURE 38.* The first normal stress  $n_{1i}$  in the two layers as functions of the network viscosity  $\eta$  of the upper layer for values of the network mobility parameter  $\alpha$  between 0.1 and 0.5. Case I where  $We_1 = 1$   $We_2 = 2$ ,  $d_1 = 0.9$   $d_2 = 0.1$ . The Newtonian viscosities are zero, the network viscosity of the lower layer is fixed at 1.

a)  $n_{11}$  vs.  $\eta_2$     b)  $n_{12}$  vs.  $\eta_2$



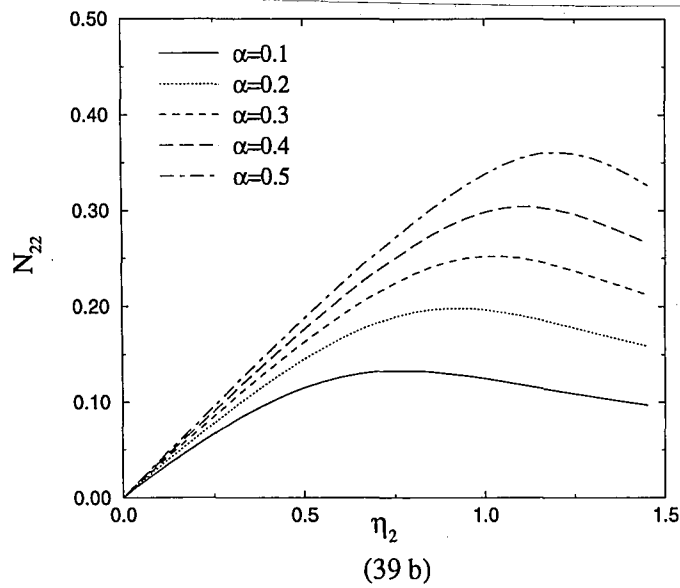
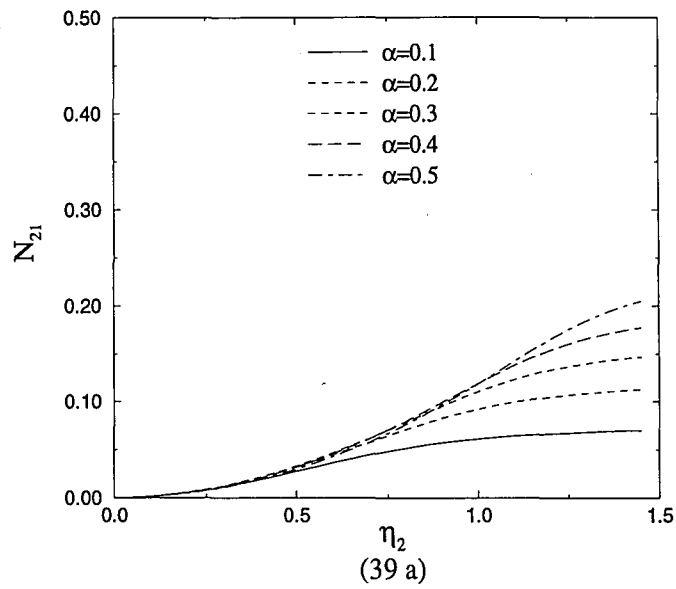


*FIGURE 39.* The second normal stress  $n_{2i}$  in the two layers as functions of the network viscosity  $\eta$  of the upper layer for values of the network mobility parameter  $\alpha$  between 0.1 and 0.5. Case I where  $We_1 = 1$   $We_2 = 2$ ,  $d_1 = 0.9$   $d_2 = 0.1$ . The Newtonian viscosity are zero, the network viscosity of the lower layer is fixed at 1.

a)  $n_{21}$  vs.  $\eta_2$     b)  $n_{22}$  vs.  $\eta_2$

## REFERENCES

- [1] Giesekus, H. "A simple constitutive equation for polymer fluids based on the concept of deformation dependent tensorial mobility", *Journal of Non-Newtonian Fluid Mechanics*, Vol 11, pp69, 1982
- [2] Yih ,C.S. "Instability due to viscosity stratification", *Journal of Fluid Mechanics*,Vol 27, pp337, 1967
- [3] Joseph, D.D. and Renardy,Y. "Fundamentals of Two Fluids Dynamics",Springer-Verlag, New york, 1992
- [4] Renardy,Y. "Stability of the Interface in two -layer Couette Flow of UCM liquids.", *Journal of Non-Newtonian Fluid Mechanics*, Vol 28 , pp 99, 1988
- 
- [5] Larson, R.G. "Instabilities in viscoelastic flows", *Rheologica Acta*, Vol 31, pp 213,1992
- [6] Bird, Rb. Curtiss, Cf. Armstrong ,R.C. Hassager O. " Dynamics of polymeric liquids 2nd ed, Vol 2. Wiley, New York, 1987
- [7] Johnson, M. and Segalman, D. "A model for viscoelastic fluid behavior which allows non- affine deformation ", *Journal of Non-Newtonian Fluid Mechanics*, Vol 2,pp 255,1977
- [8] Phan-Thien and Tanner ."A new constitutive equation derived from network theory",*Journal of Non-Newtonian Fluid Mechanics* , Vol 2, pp353, 1977
- [9] Phan-Thien. "A Nonlinear Network Viscoelastic Model", *Journal of Rheology*, Vol 22, pp 559, 1978
- [10] Larson ,R.G. "Convection and Diffusion of Polymer Network Strands", *Journal of Non-Newtonian Fluid Mechanics*, Vol 13, pp279, 1983

[11] Larson ,R.G. "A Constitutive Equation for Polymer Melts Based on Partially Extending Strand Convection", Journal of Rheology, Vol 22,pp 545, 1984

## VITA

Mukaddes Selviboy was born on December 14 th , 1970 in Eskisehir, Turkey. She received her B.S. degree in Mathematics at Anadolu University of Eskisehir in 1992. Having worked in Eskisehir Yediler Adim preparation school for one year as a Mathematics teacher, she started working as a research assistant at Sakarya University of Adapazari in 1993. She started her studies in pursuit of the M.S. in the Applied Mathematics division of Mechanical Engineering Department in 1994 at Lehigh University, USA. She holds a position at Sakarya University of Adapazari.

---

**END  
OF  
TITLE**